

The bright Ly α side of the high-redshift Intergalactic Medium

Sebastiano Cantalupo

Kavli Institute for Cosmology Cambridge & Institute of Astronomy

Collaborators: Simon J. Lilly (ETH Zurich), Cristiano Porciani (AlfA Bonn)

Outline

- Brief introduction and motivations
- Detecting the Intergalactic Medium (IGM) at $z \sim 3$ with **fluorescent Ly α emission**:
 - theoretical models
 - observational results
- Mapping HI during the Epoch of **Reionization (EoR)** with the **Ly α emission from QSO I-fronts**
 - basic idea
 - radiative transfer model
 - recent numerical results
 - detectability
- Bonus track: local photoionization flux, gas cooling and galaxy formation

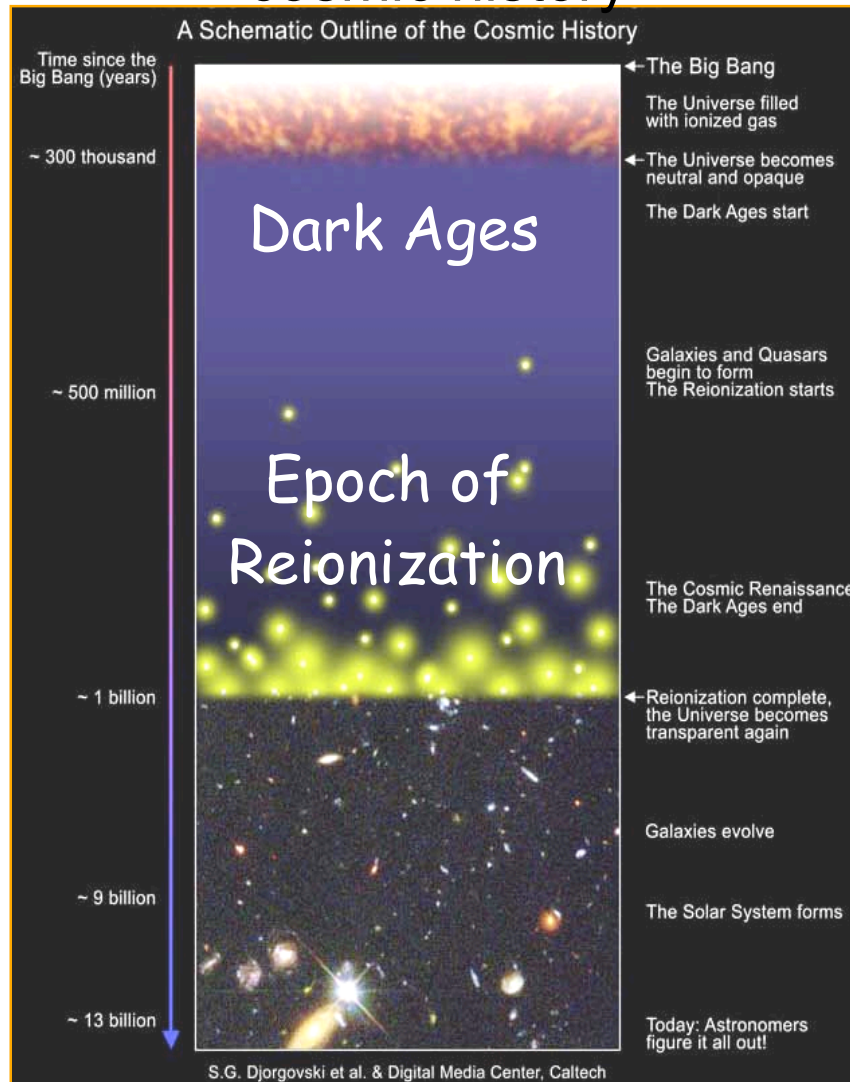
Why to study the IGM?

The followings are just **few** reasons:

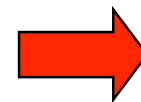
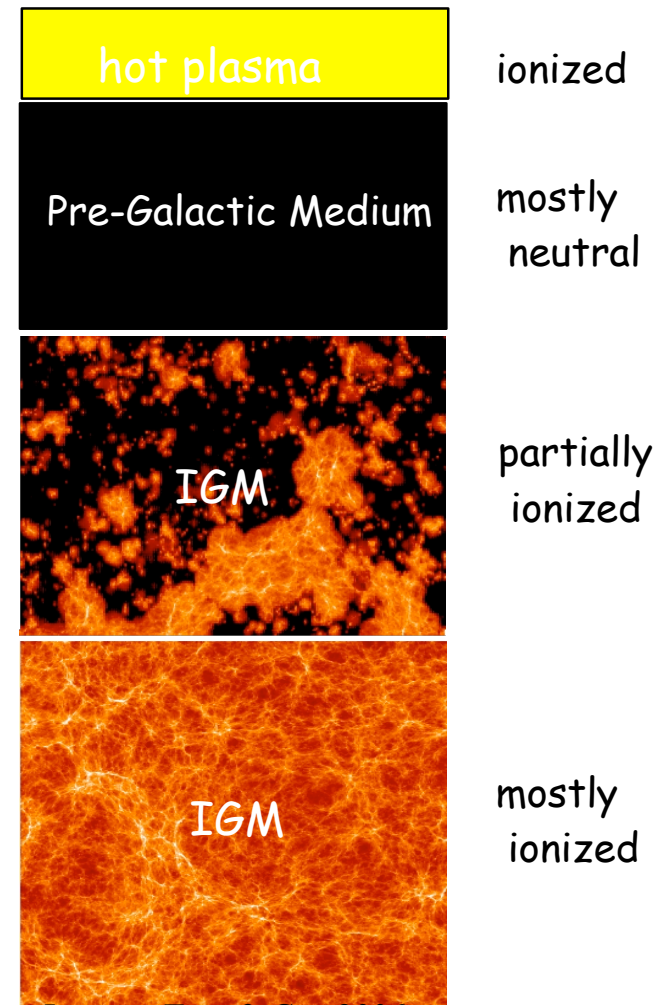
- it is where most of the **baryons** are
- trace well the **Large Scale Structure** of the Universe
- closely connected to the **first steps** of **galaxy formation** but easier to model/understand (less unconstrained physical processes)

What do we know about the IGM?

cosmic history

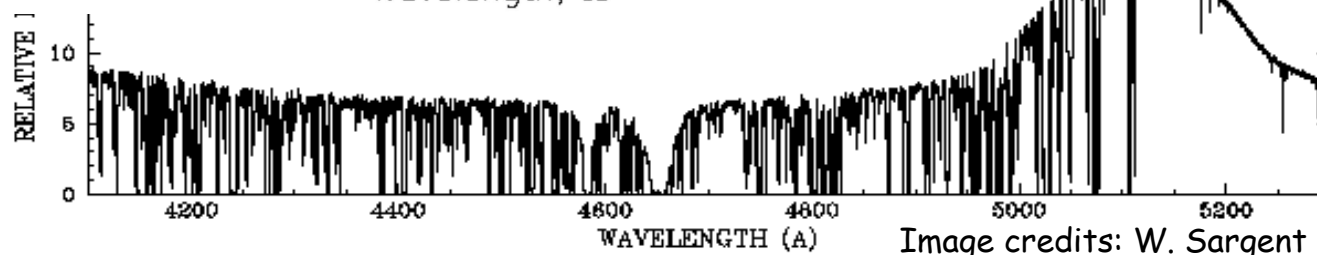
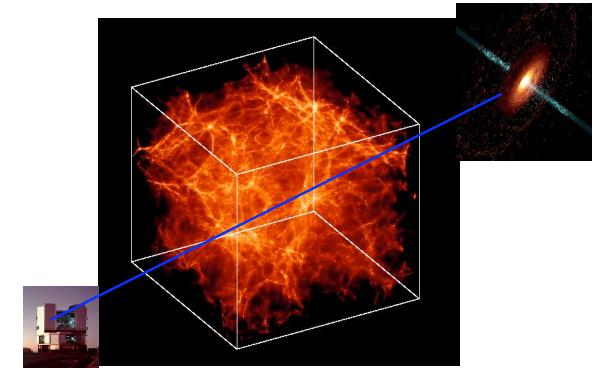
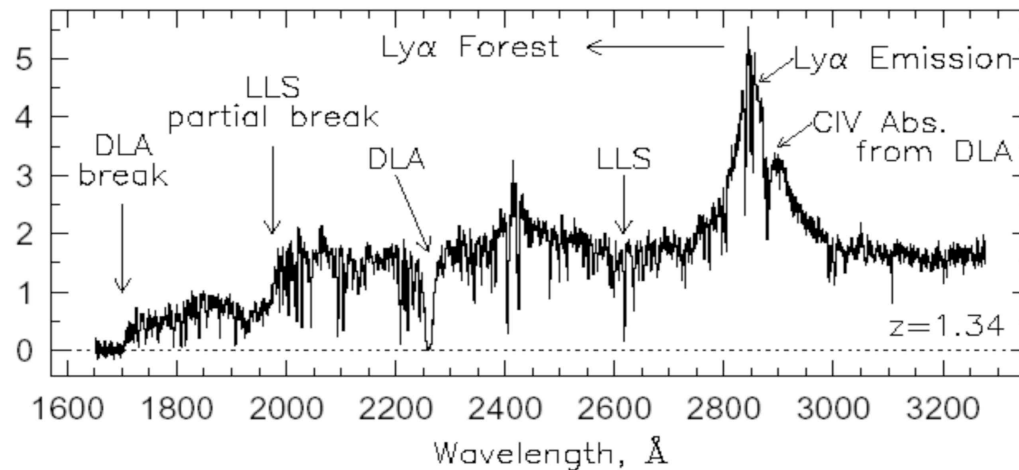


cosmic hydrogen history



Images: Trac & Cen 2006

Classical approach to study the IGM: in absorption



- powerful tool to map also the low-density (ionized) gas and **to constrain cosmology**
- However: **only 1D** information on **denser** (mostly neutral?) **HI clouds** (e.g., LLSs)

What we would like (still) to know about the post-Reionization IGM:

where is the neutral IGM?

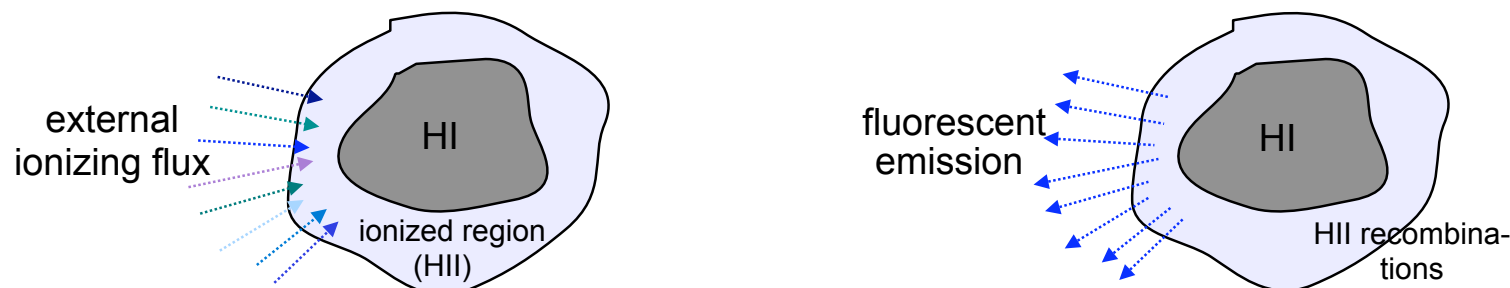
i.e., what is the nature of the **LLSs** (and DLAs)?

do they exist **HI clouds** in the IGM **without** significant star-formation (**proto-galactic** clouds or “**dark galaxies**”)?

How the galaxies get their gas from the IGM (cold/hot, streams/smooth, etc.)?

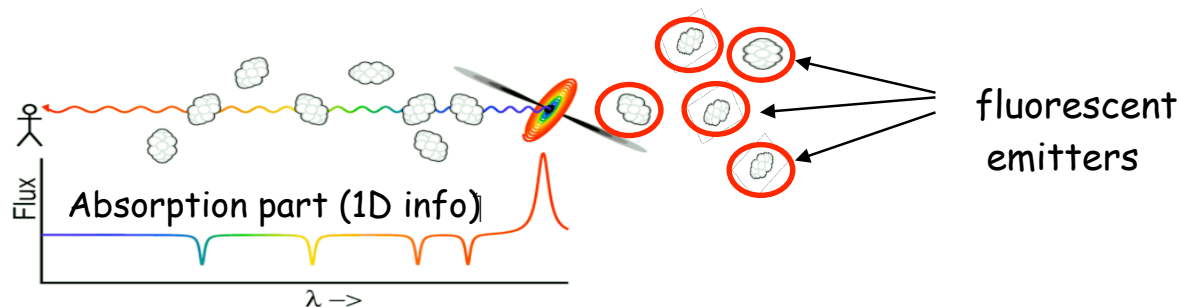
Fluorescent Ly α emission at $z \sim 3$: basic idea and motivations

→ **Self-shielded HI clouds** re-emit a significant fraction of the impinging ionizing flux in Ly α (via **HII recombinations**) (Hogan & Weymann 1987; Gould & Weinberg 1996).



→ Advantages:

- **2D** information



- Ly α SB is **proportional** to the external ionizing flux, therefore:

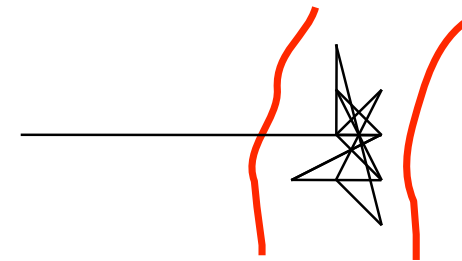
- we can **measure the UV background**
- knowing the ionizing flux (e.g., from a QSO) we can **exclude** clouds with internal **star-formation**
- if the source is a QSO: we can get the **QSO age** and **angular** shape of the emission

How to **model** fluorescent Ly α emission?

high optical depth (to escape the medium) $\sim 10^4$ - 10^5

“random walk” in space and frequency

➔ **Monte Carlo** techniques

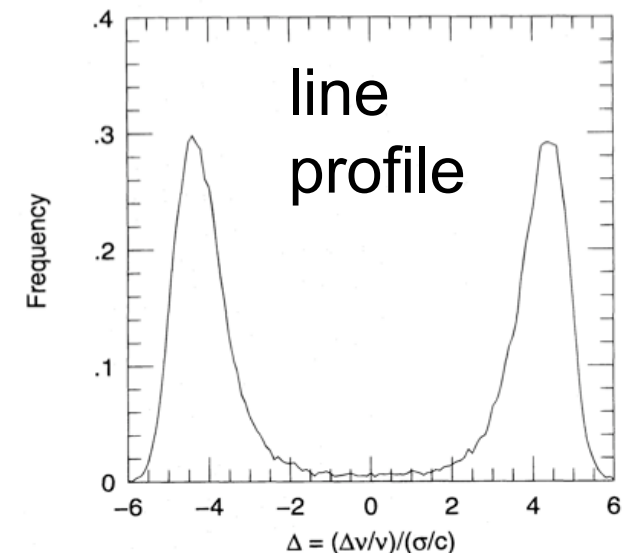


early works based on:

- ➔ homogeneous **slab** approximation (e.g., Gould & Weinberg 1996)
or isothermal sphere (Zheng & Miralda-Escude' 2002)
- ➔ **static** or rotating cloud
- ➔ uniform (external) illumination

main **results**:

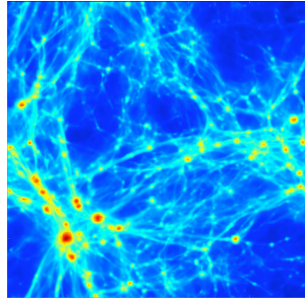
- ➔ **uniform** Ly α SB ($\sim 60\%$ of impinging ionizing flux)
- ➔ **double peaked** line profile



Gould & Weinberg 1996

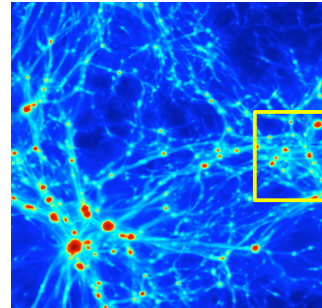
Our approach:

Hydrogen distribution



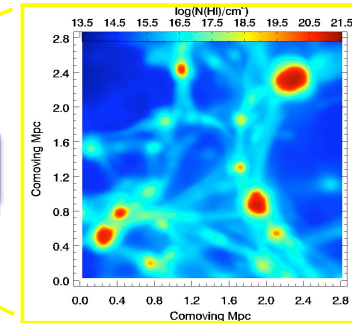
**continuum RT
(ionizing radiation)**

Neutral Hydrogen

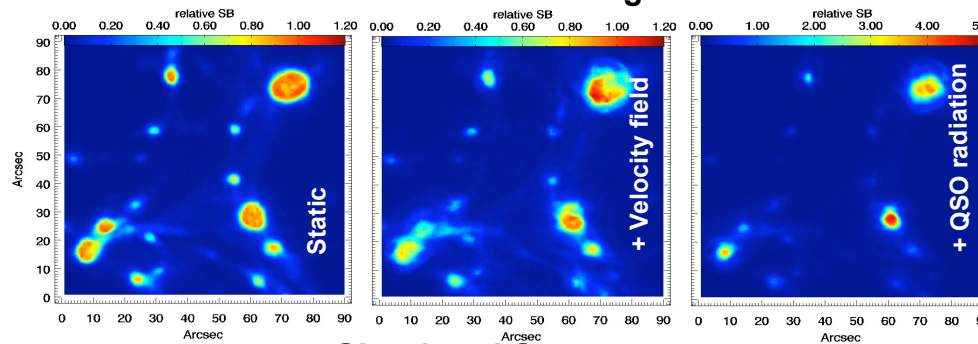


**Grid
refinement**

Refined HI distribution



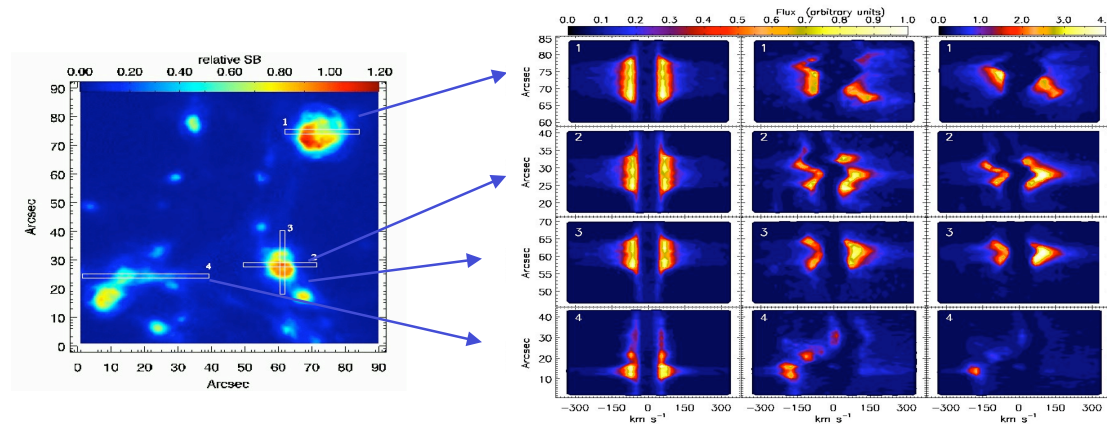
Simulated images



**Ly α
Monte Carlo RT**

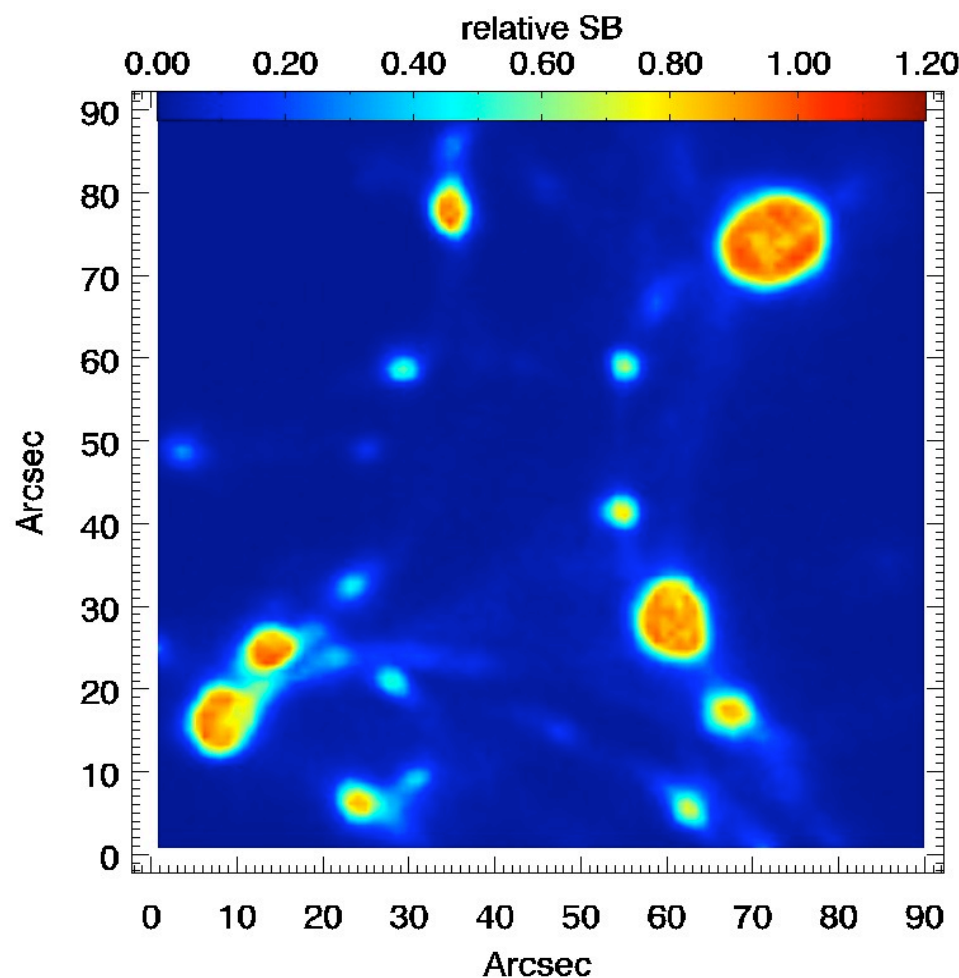


Simulated Spectra

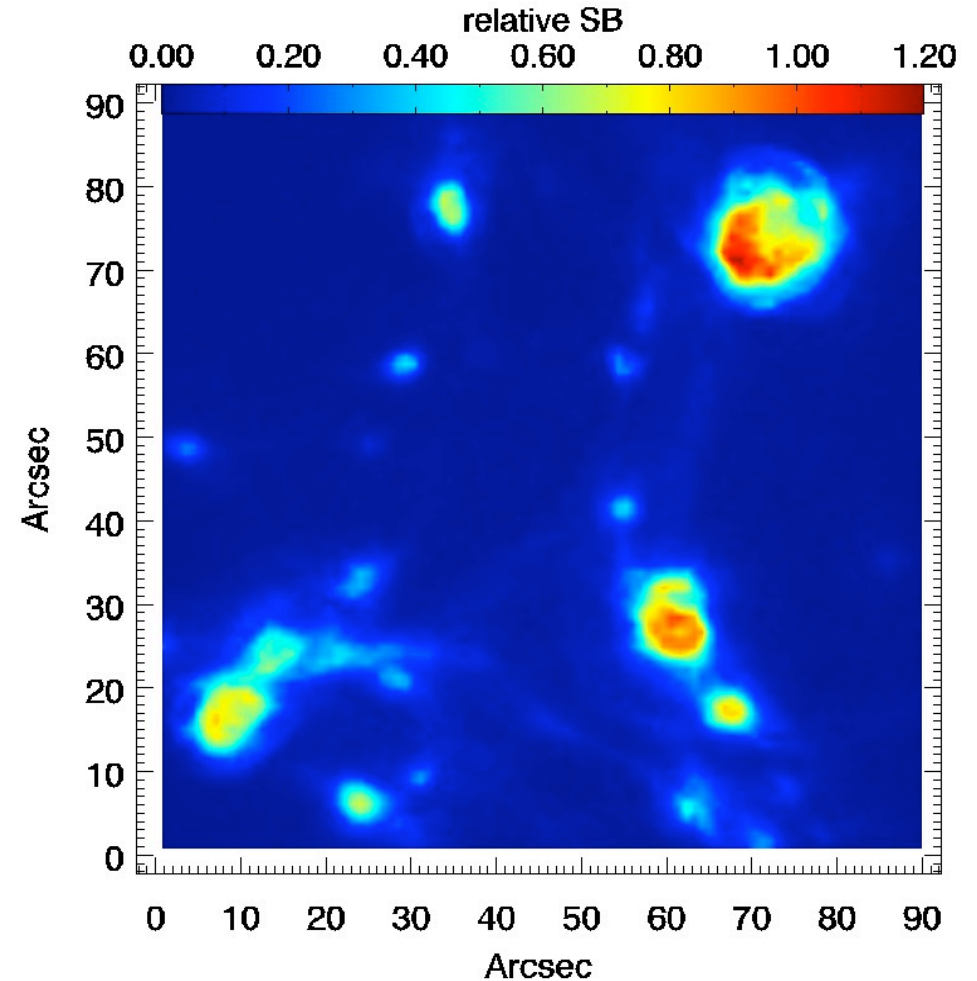


SC, Porciani, Lilly & Miniati 2005

Results: Ly α images and the effect of the gas velocity field



Static Case

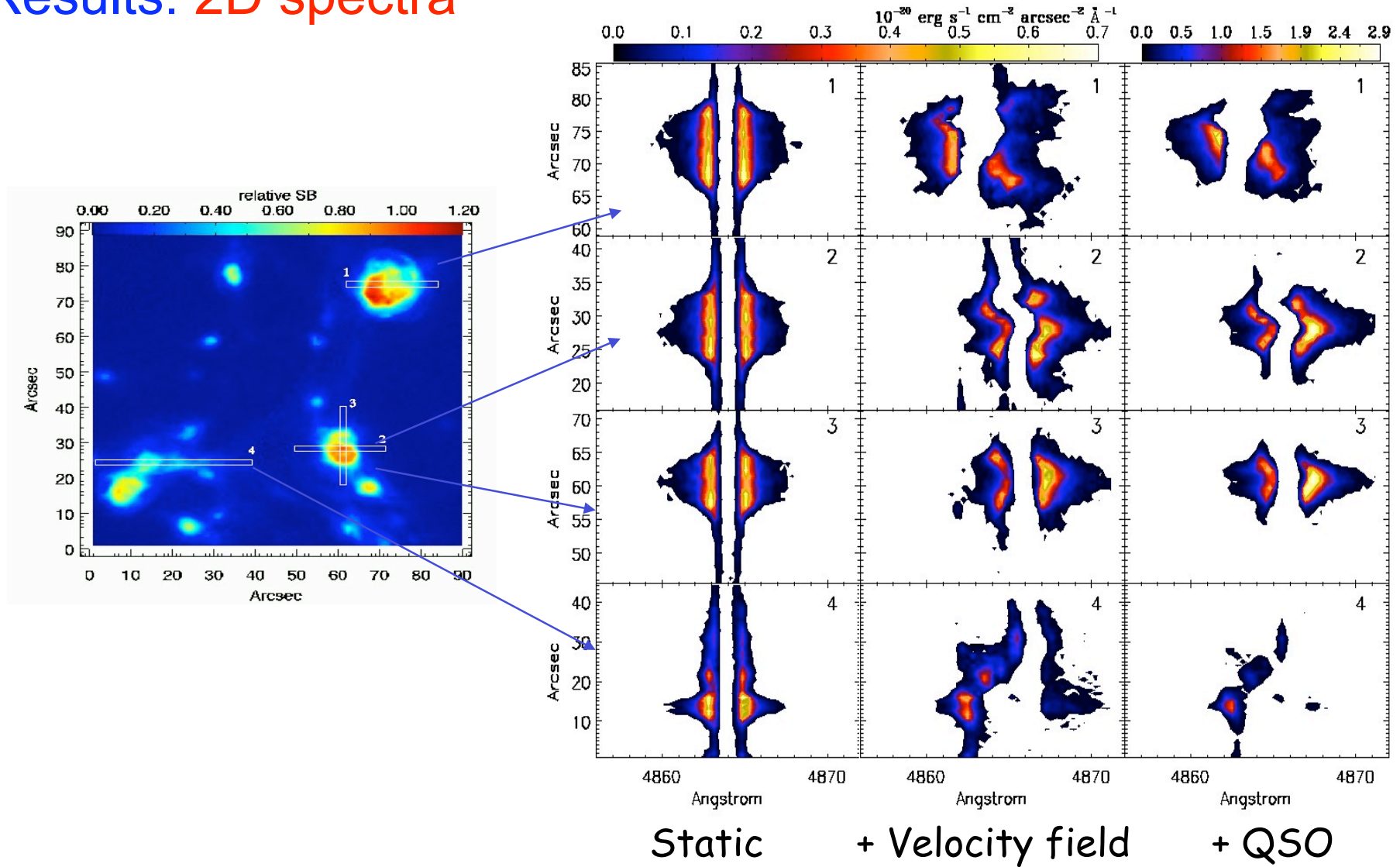


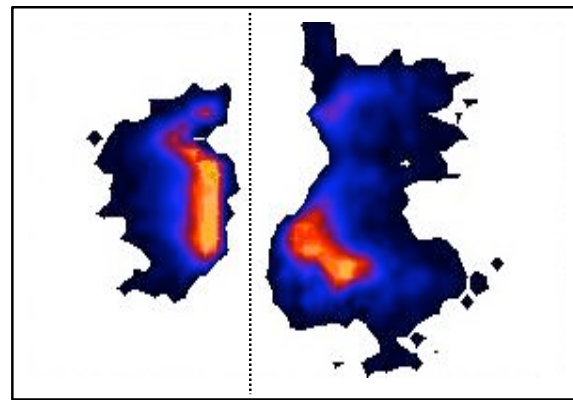
Including velocity field

Surface-Brightness relative to:

$$SB_{HM} = 3.67 \times 10^{-20} \text{ ergs cm}^{-2} \text{ s}^{-1} \text{ arcsec}^{-2}$$

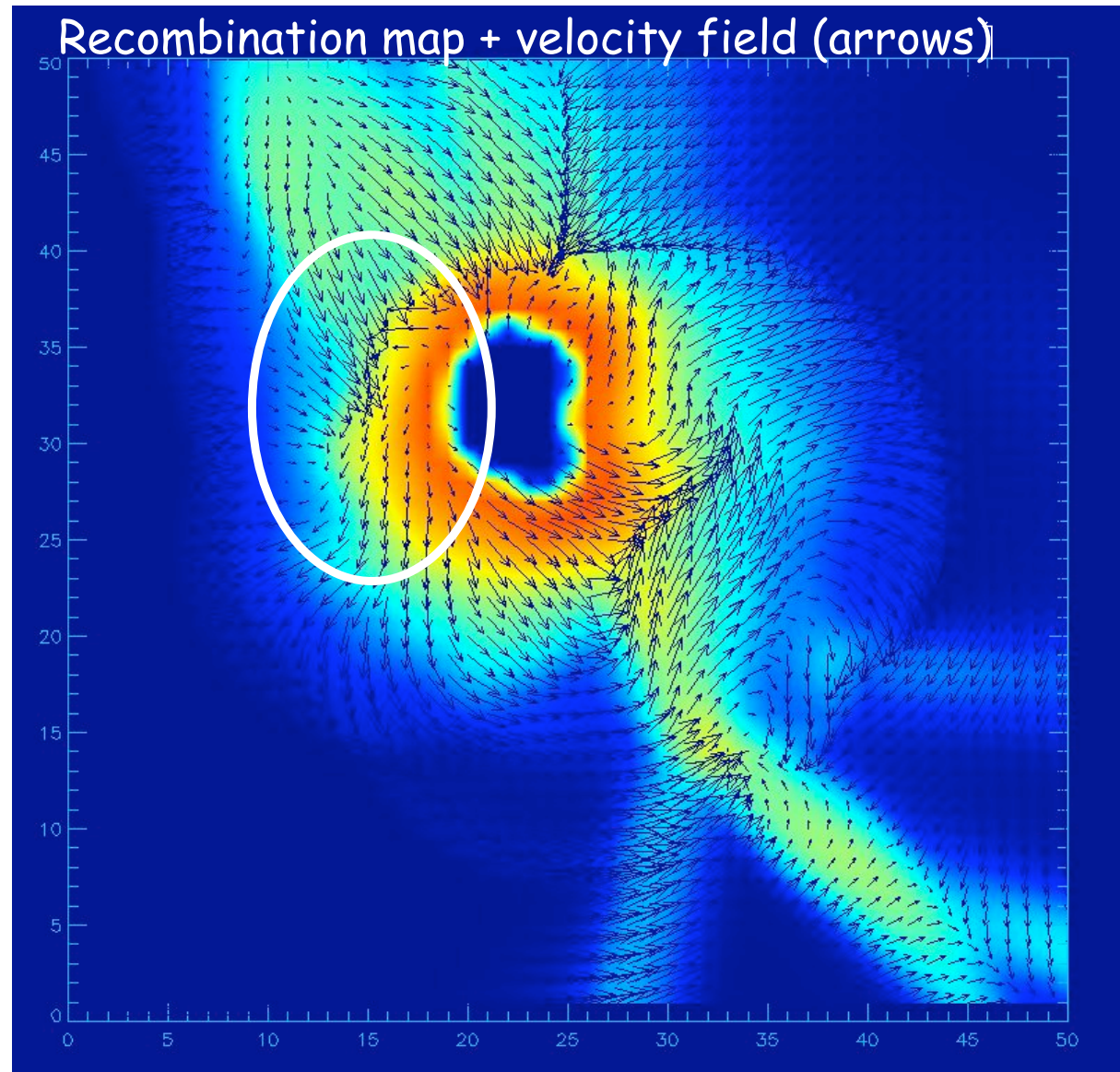
Results: 2D spectra





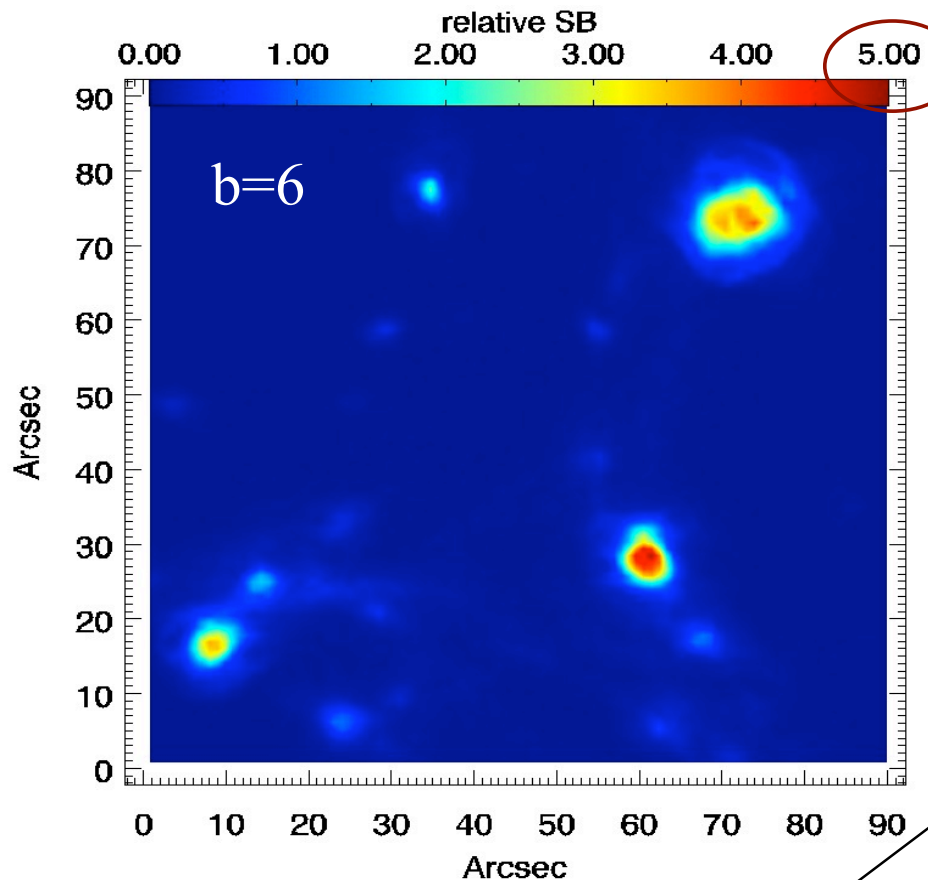
wavelength

Slit coordinate



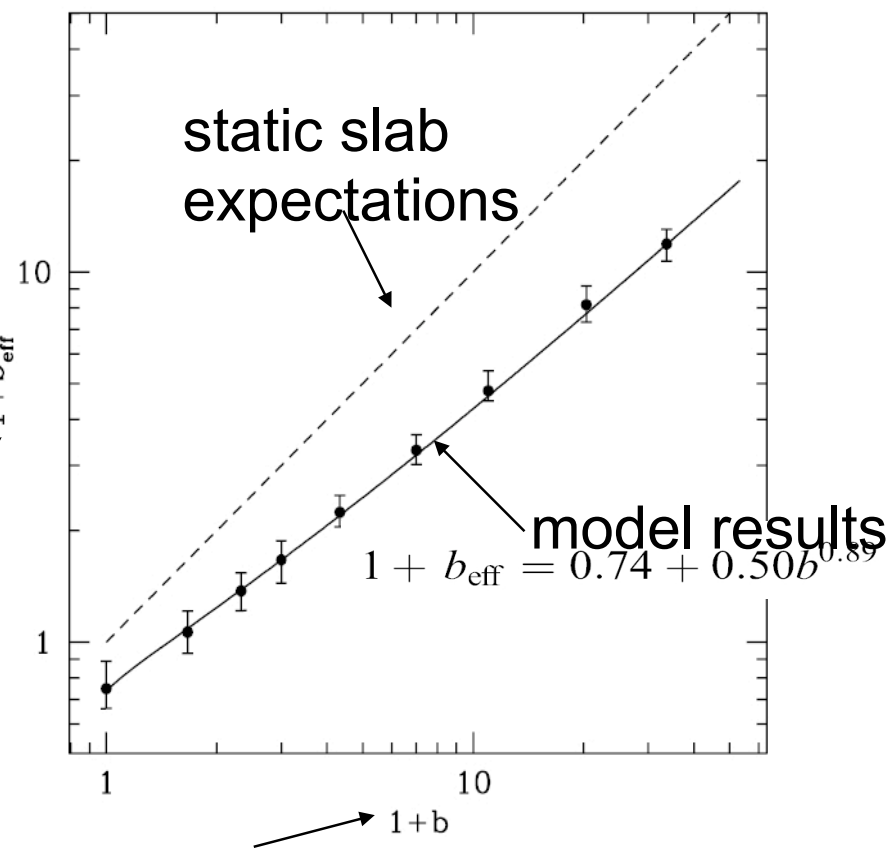
depth

Adding the QSO flux: the “geometrical” effect



1+b=7
expected!

effective “boost factor” from the observed SB
 $SB_{||} = (1 + b_{\text{eff}})SB_{\text{HM}}$.



input “boost factor” from QSO

Is it **detectable**?

fluorescence from cosmic UV-background
below the **limit** for current facilities.

BUT using a **QSO** for boosting fluorescence
should make the first detection possible.

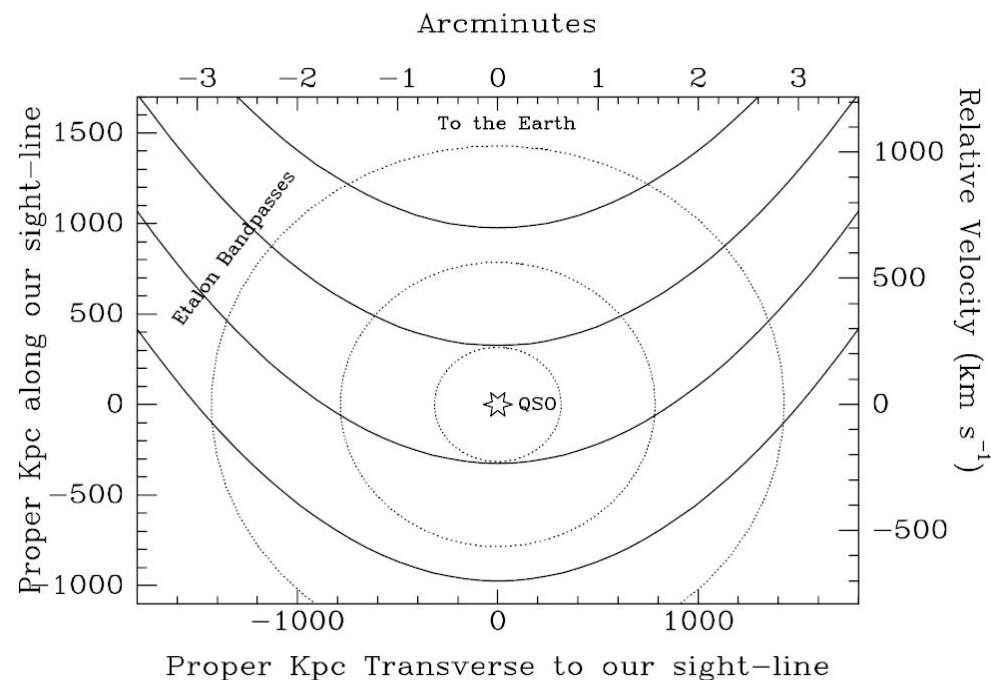
Let's look at all the attempts to detect this
emission so far...

First attempt: Tunable-Filter search around a QSO at $z=2.17$
Francis and Bland-Hawthorn 2004

expectation based on **slab model**
(6 clouds with 100 arcsec^2)

result: **null detection**

result **consistent** with our
model (expected 0.3 clouds in
the survey volume).



main reasons: too small volume, expected size and
number density decrease in proximity of the QSO.

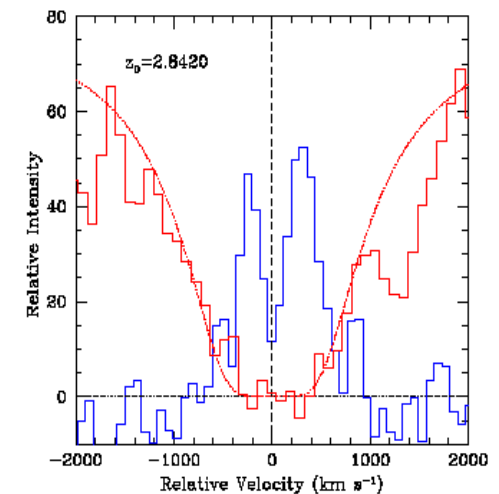
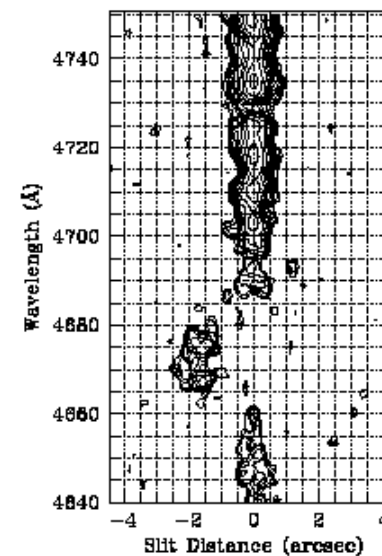
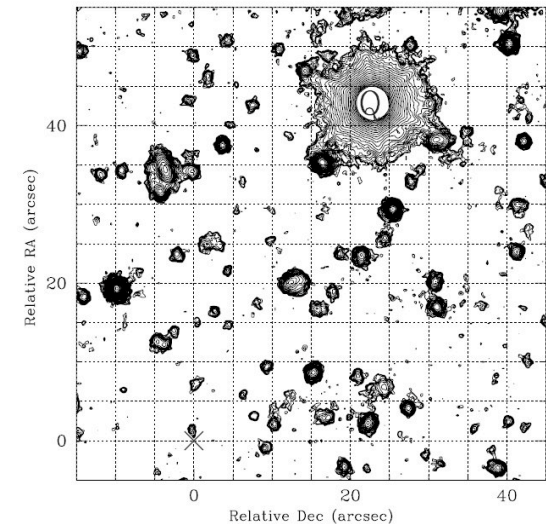
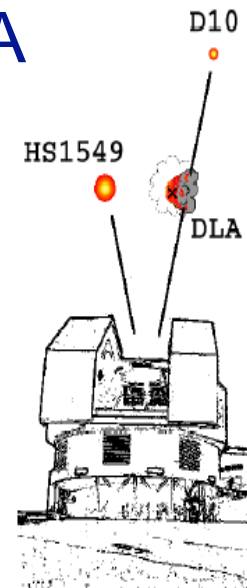
Possible fluorescence from a DLA

(Adelberger et al. 2006)

serendip. discovered: double peaked line profile, SB consistent with fluorescence (?)

problems: continuum detected (in G and R band, ~26 mag), metal lines, very close to the QSO (unrealistic size to be self-shielded)

most likely there is star formation inside. Ly-alpha galaxy?



Integral-field spectroscopy search around a QSO at $z \sim 4$

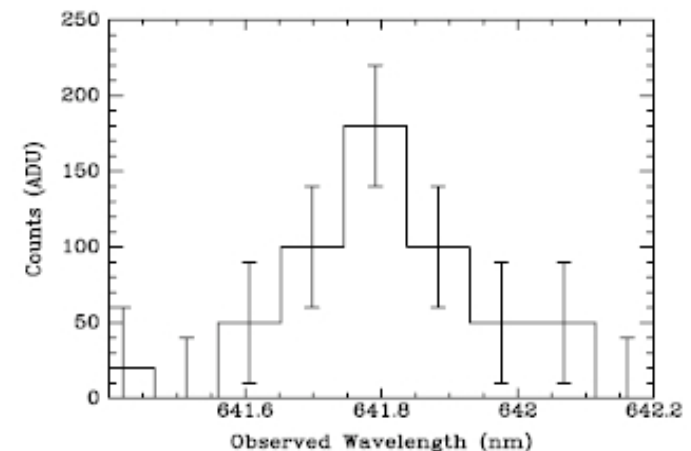
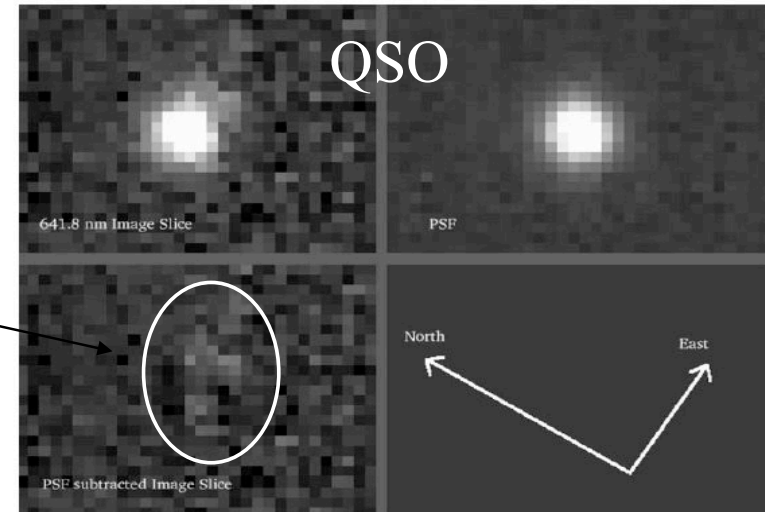
Francis & McDonnell 2006

detection of 1 Ly-alpha emission around the QSO (?)

problems: just 50Kpc from QSO (physically connected?)

no constraints on SB or EW (because of QSO subtraction)

technique limitation: very small volume sampled.



Our approach: blind search with **multislit+filter** technique

4 Nights @ VLT-FORS2

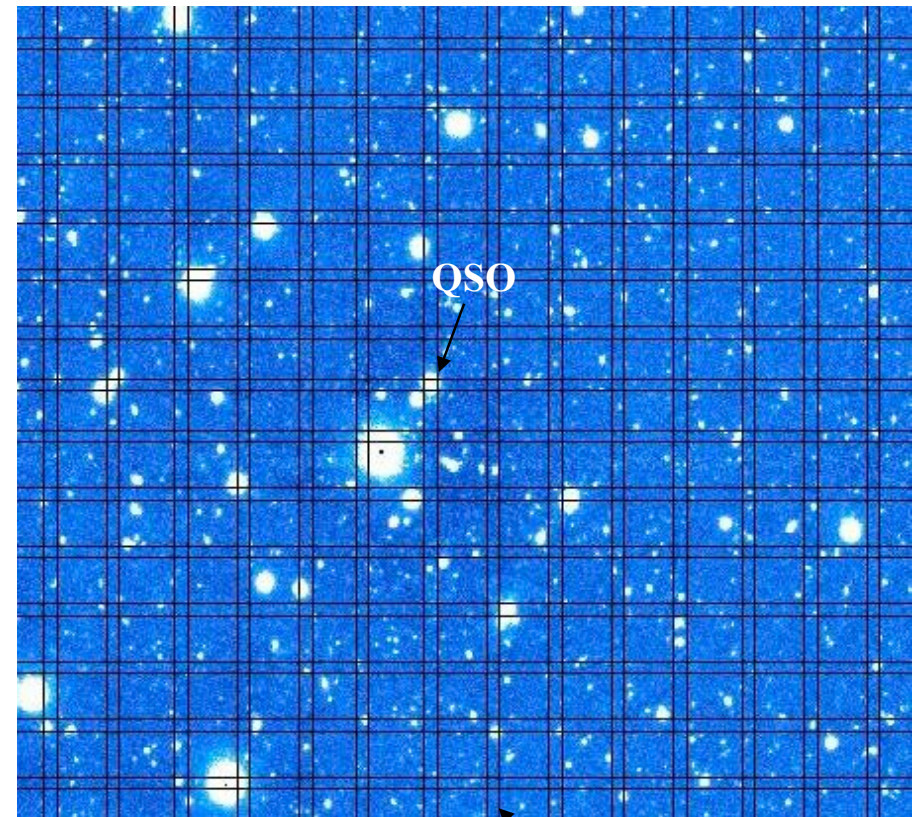


Target: **$z=3.1$ QSO** 0420-388
(**brightest** QSO in FORS2 narrow filters)

14 slits (2"x7')

2 filters + 2 mask rotations
+ 1 deep V-band image

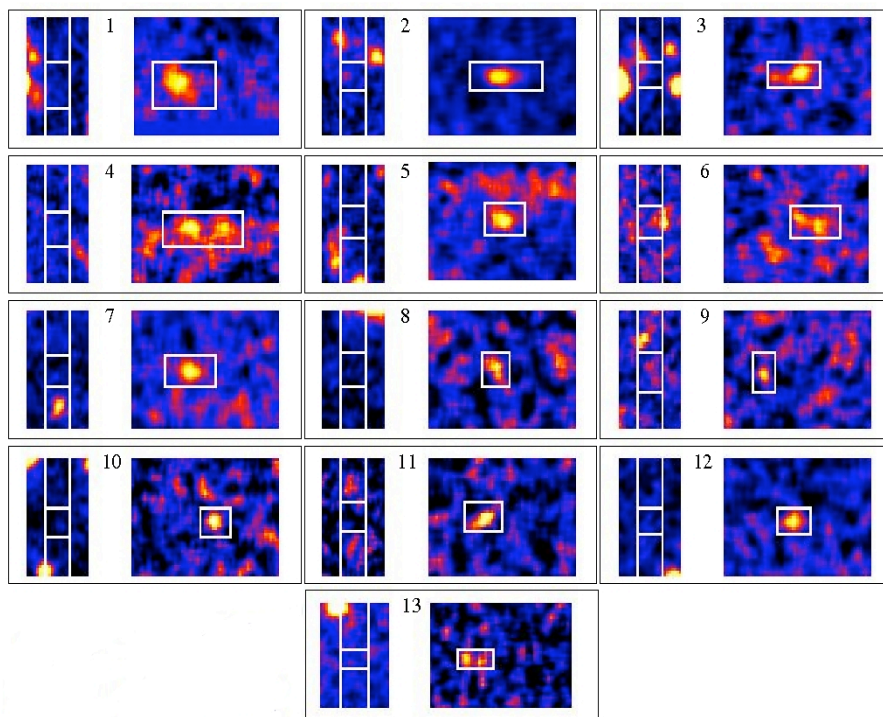
(sparsely) sampled volume=**14000 comoving Mpc³**
expected #: ~7-10 fluorescent emitters



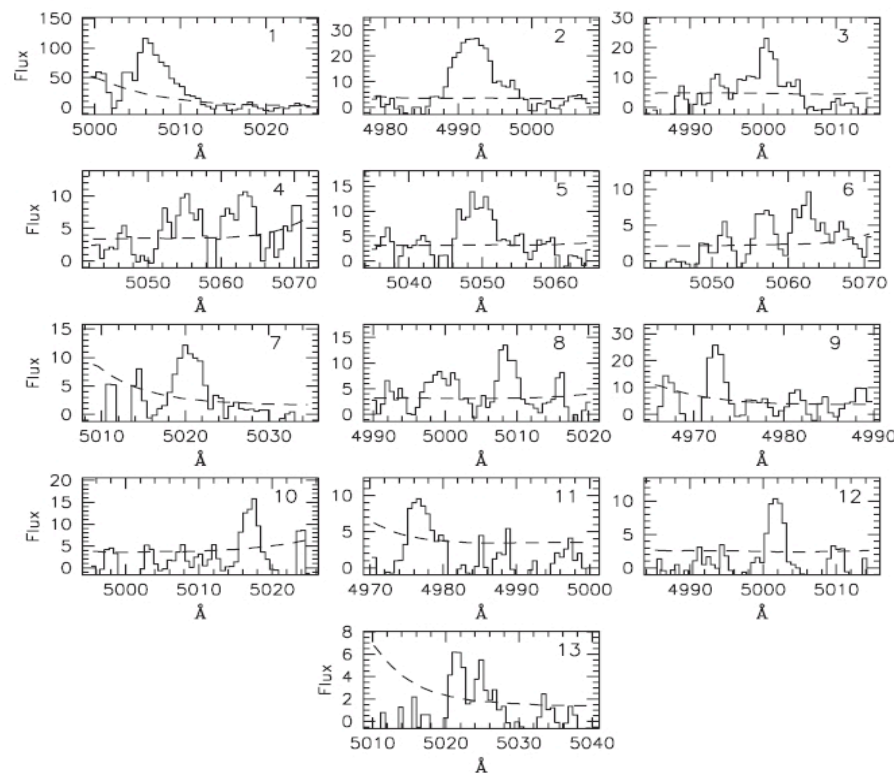
slits

SC, Lilly & Porciani 2007

Results: 13 Ly α candidates detected

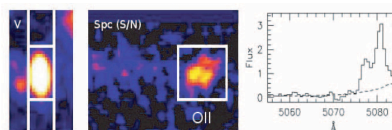


slit positions (V image) and 2D spectra



1D spectra

+ 2 OII interlopers ($z \sim 0.7$), e.g.:



Are they fluorescent or galaxies?

primary constraints:

- equivalent width (EW)
- SB – distance relation

secondary constraints:

- line profile
- number density

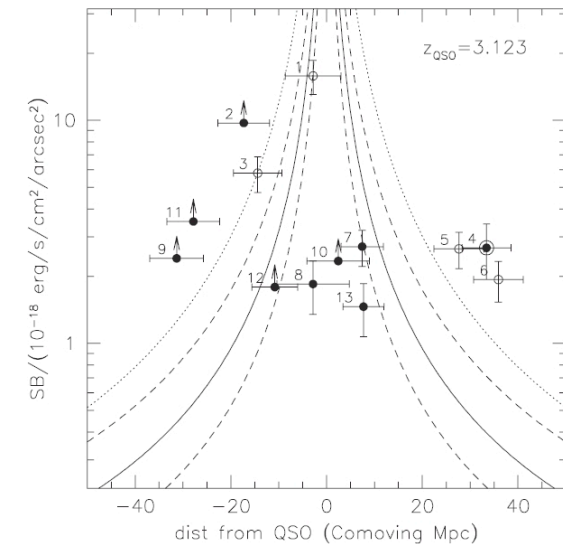
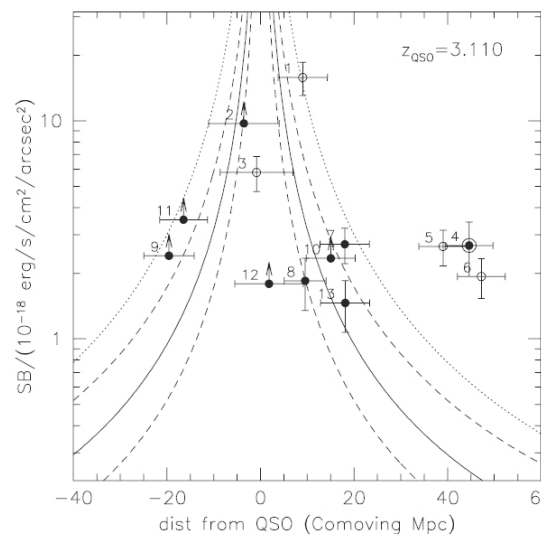
they all indicate that about half of them are plausibly fluorescent

further studies (e.g., increasing EW constraint) are needed...

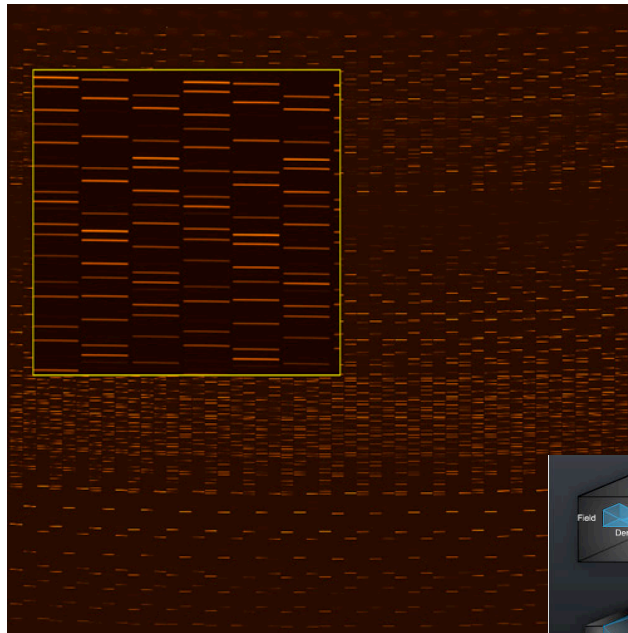
TABLE 3
SPECTROPHOTOMETRIC PROPERTIES OF THE Ly α CANDIDATES

OBJECT NUMBER	$F_{\text{line}} \pm 1 \sigma$ (10^{-18} ergs s^{-1} cm^{-2})	$f_{\text{r}} \pm 1 \sigma$ (10^{-20} ergs s^{-1} cm^{-2} \AA^{-1})	EW ₀ (\AA)	SB (10^{-18} ergs s^{-1} cm^{-2} arcsec^{-2})	FLUORESCENT? ^a		
					EW	EP	SB
1.....	58.27 ± 6.67	6.55 ± 5.90	≥370	15.81 ± 2.73	+		+
2.....	18.81 ± 1.20	3.43 ± 3.69	>150	≥9.72	+		+ ^b
3.....	12.98 ± 1.35	16.70 ± 3.32	16 $^{+9}_{-4}$	5.80 ± 1.06	-		+
4.....	11.33 ± 1.41	1.46 ± 4.43	>65	2.68 ± 0.78	+	+	-
5.....	7.30 ± 0.81	4.76 ± 4.06	≥36	2.65 ± 0.49			-
6.....	6.36 ± 0.68	8.86 ± 4.06	15 $^{+17}_{-5}$	1.93 ± 0.40	-		+
7.....	5.31 ± 0.82	0.86 ± 4.06	>30	2.71 ± 0.50			+
8.....	4.70 ± 0.67	0.59 ± 4.43	>24	1.84 ± 0.49			+
9.....	4.21 ± 1.16	0.65 ± 5.17	>18	≥2.40			-
10.....	4.06 ± 1.01	-5.65 ± 3.69	>25	≥2.34			+
11.....	3.49 ± 1.05	-1.98 ± 3.69	>21	≥3.52			-
12.....	2.65 ± 0.56	3.17 ± 3.32	>18	≥1.79			+
13.....	2.62 ± 0.45	2.34 ± 2.58	>23 (>70) ^c	1.46 ± 0.39		+	+
Previous Fluorescent Ly α Candidates in the Literature							
AA1 ^d	21.0 ± 5.0		72 $^{+20}_{-20}$	110.00 ± 26.00	-		+
FD1 ^e	≥15.0		>19				

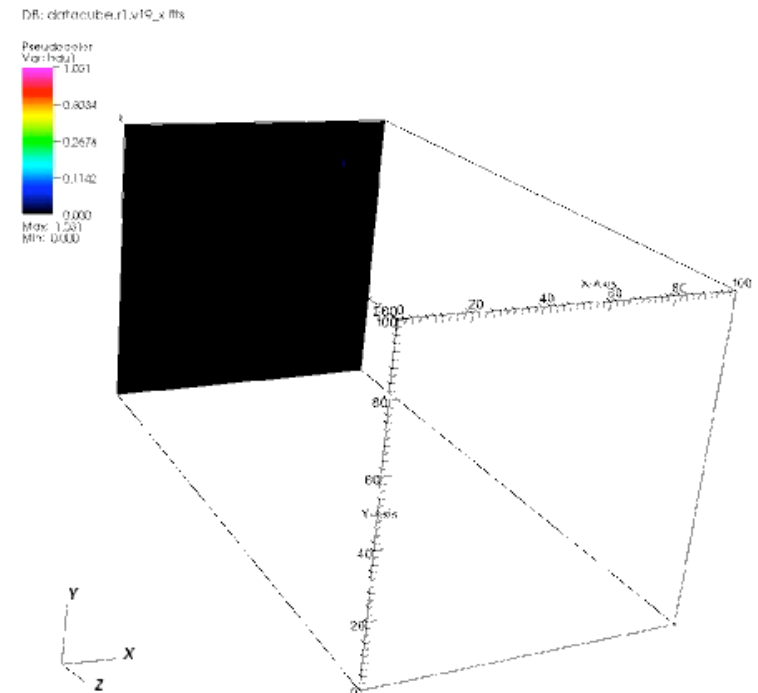
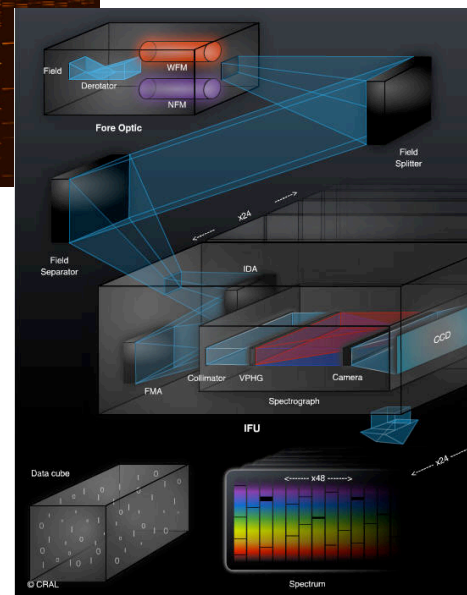
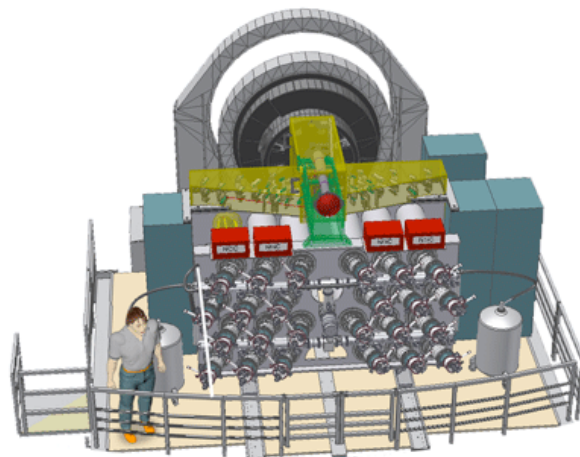
^a In view of the indicators discussed in § 2 (where EP = emission-line profile).
^b If $z_{\text{QSO}} = 3.110$.
^c If the line is O II at $z = 0.36$.
^d Adelberger et al. (2006); candidate at $z = 2.842$.
^e Francis & McDonnell (2006); candidate at $z = 4.279$.



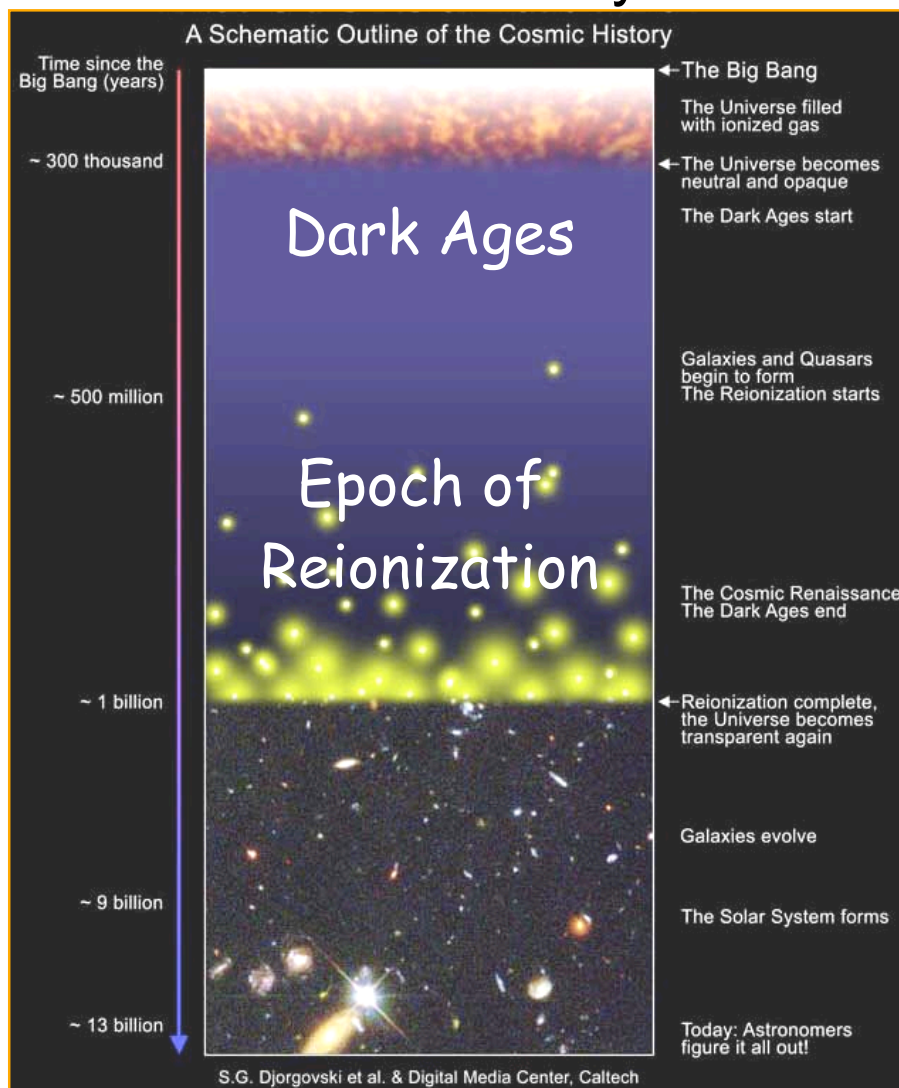
Next future (2012): **MUSE** (Multi-Unit Spectroscopic Explorer) @ VLT



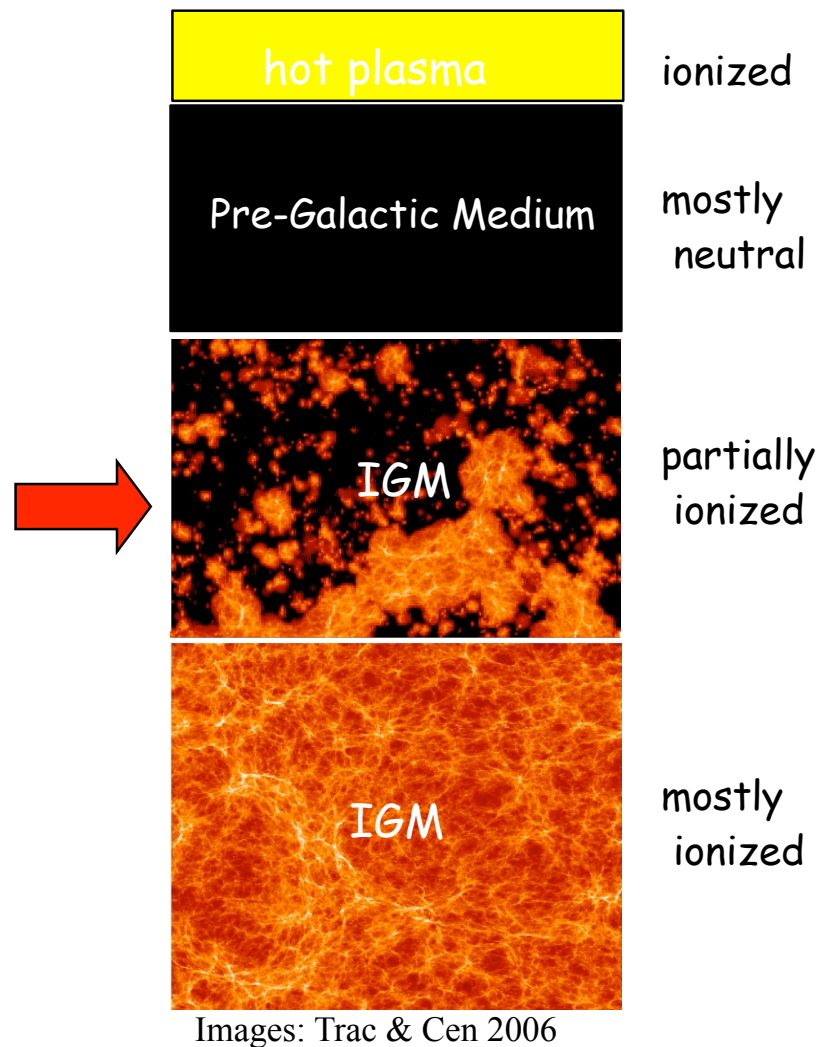
- 1'x1' Integral Field Unit
- 24 modules, 3750 spectra each (!)
- range: 4800-9200 Å (z~3-6.5 for Ly α)
- Adaptive Optics



cosmic history



cosmic hydrogen history



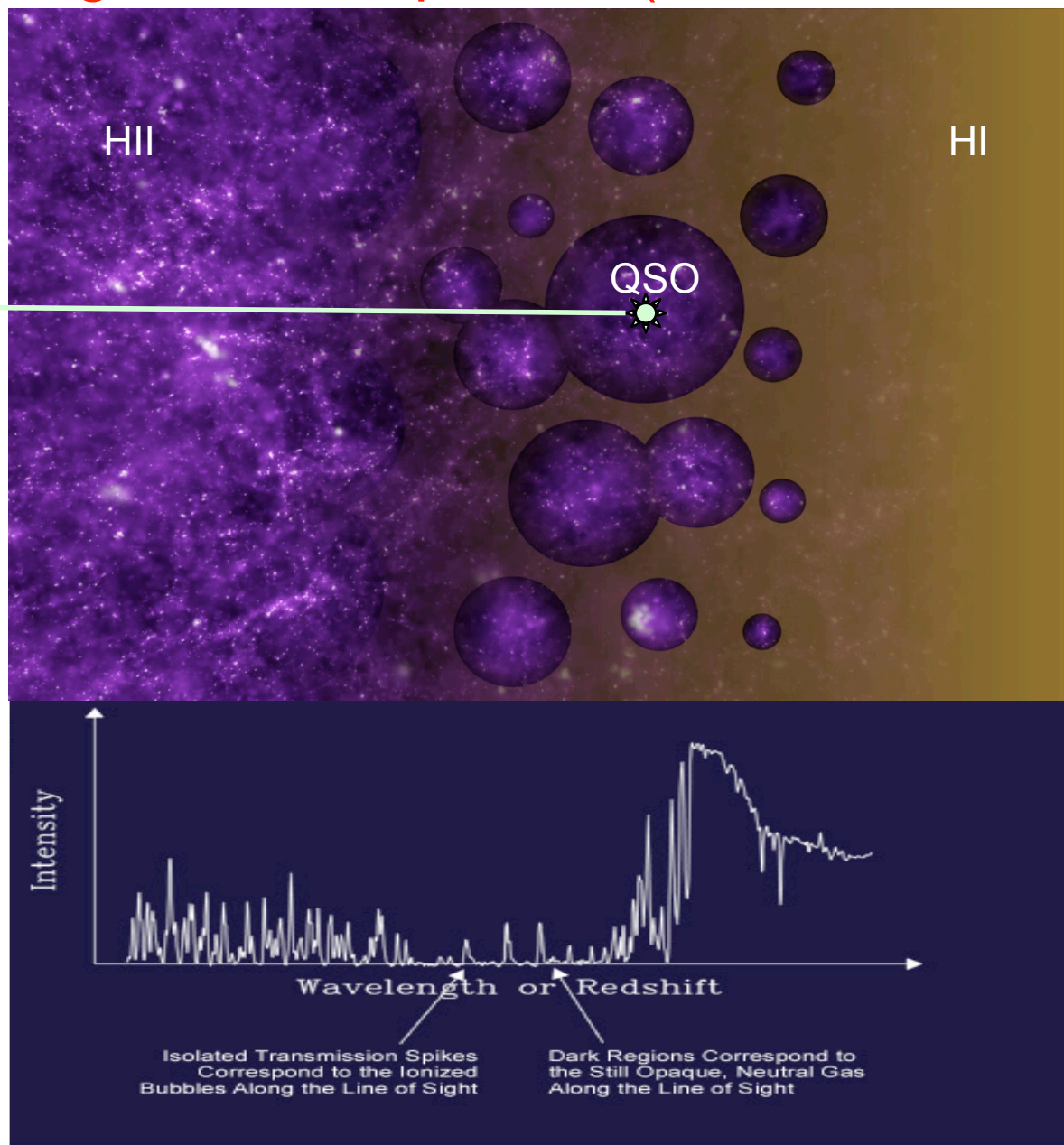
Reionization F.A.Q.

- Q1: **When** did happened?
- Q2: **How?** (i.e., who did the job?)
- Q3: Should we really care about Q1 and Q2?

Yes, if you are also interested in:

- > the **physics** of the (post-EoR) **Intergalactic Medium**
- > understanding (the first steps of) the **galaxy-formation** process
- > measuring **cosmological parameters** (e.g., with **CMB** large-scale polarization or galaxy power-spectrum)
- > **answer** to fundamental questions
- > **finding** new questions

Constraints (1): high-redshift quasars (Gunn-Peterson effect)



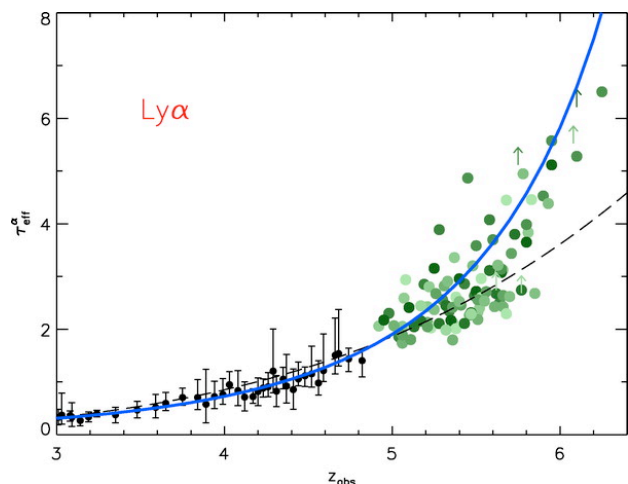
Constraints (1): high-redshift quasars (Gunn-Peterson effect)

$$t_{GP} \approx 6 \times 10^5 x_{HI} \left(\frac{1+z}{10} \right)^{3/2}$$

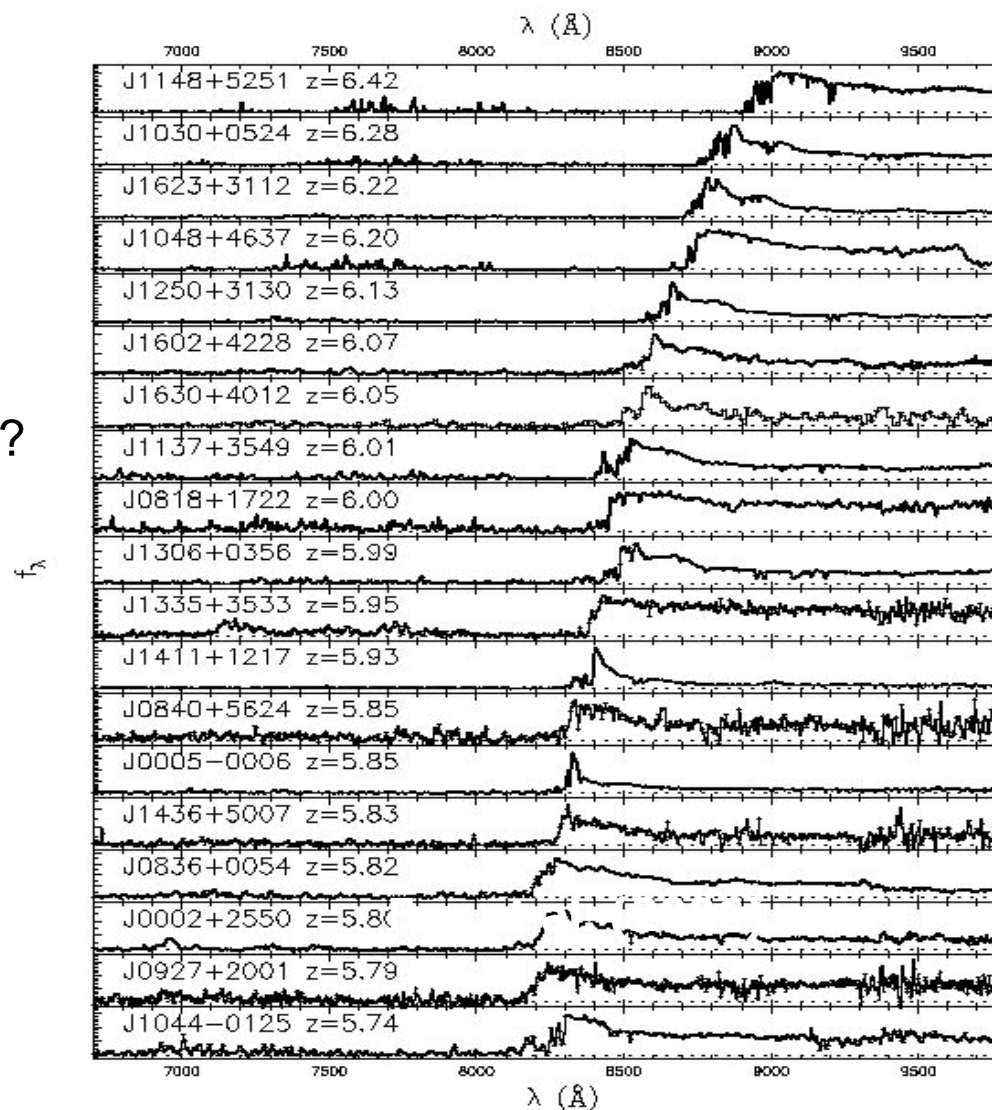
main limitation:

- Saturates already at very low neutral fractions (0.0001)

probing only the **END** of reionization?



Becker et. al 2007



Fan et. al 2006

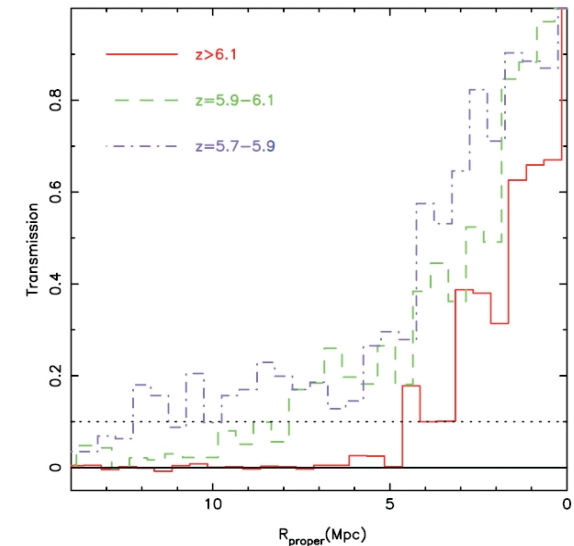
Constraints (2): HII region size in QSO spectra

bubble size related to mean HI fraction (f_{HI}):

$$R_s = 8.0 f_{\text{HI}}^{-1/3} (\dot{N}_Q / 6.5 \times 10^{57} \text{ s}^{-1})^{1/3} (t_Q / 2 \times 10^7 \text{ yr})^{1/3} \times [(1 + z_Q) / 7]^{-1} \text{ proper Mpc.} \quad \text{for } t \ll t_{\text{rec}}$$

(Haiman 2002)

... but we need (also) the QSO **age** to constrain f_{HI} .

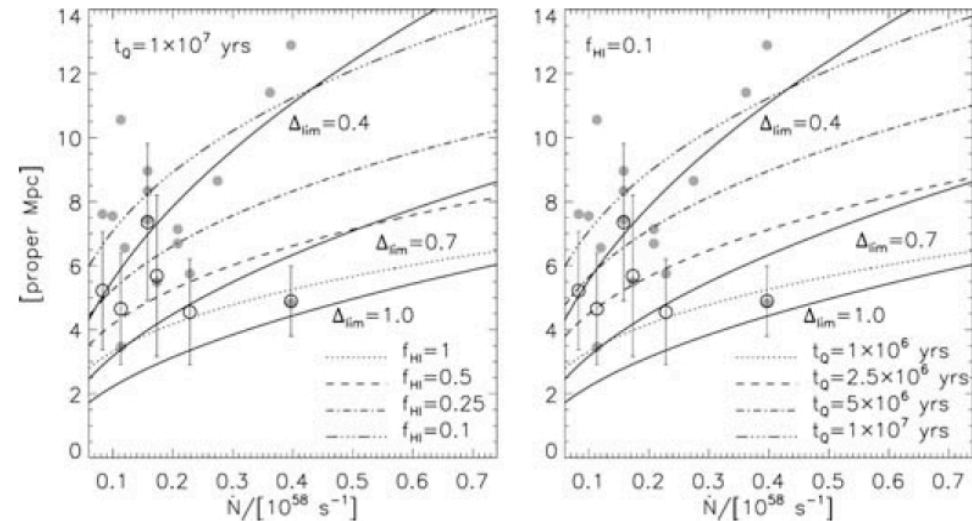


Fan et al. 2006

Again: **hint** for rapid redshift evolution,

but **no clear** values for the HI fraction

(see e.g., White+ 2003; Whythe+ 2005; Yu & Lu 2005; Bolton & Haehnelt 2007; Maselli+2007)



from Bolton & Haehnelt 2007

Constraints (3): Ly α galaxies (LF and clustering evolution)

Basic idea:

IGM **transmission** changes Ly α galaxies **Luminosity Function** (Miralda-Escude' 1998) and **clustering** (McQuinn+ 2007).

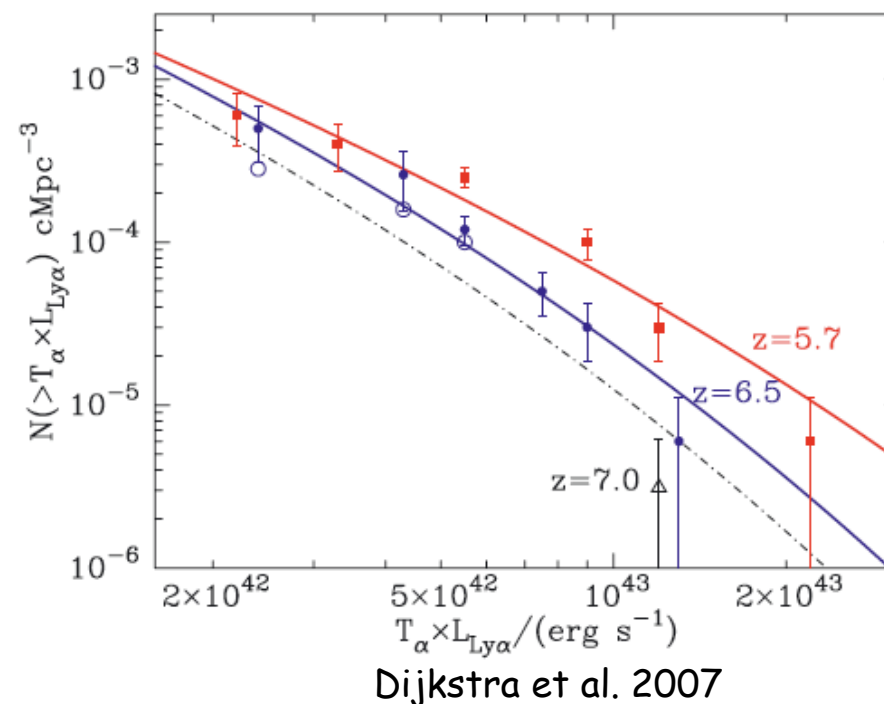
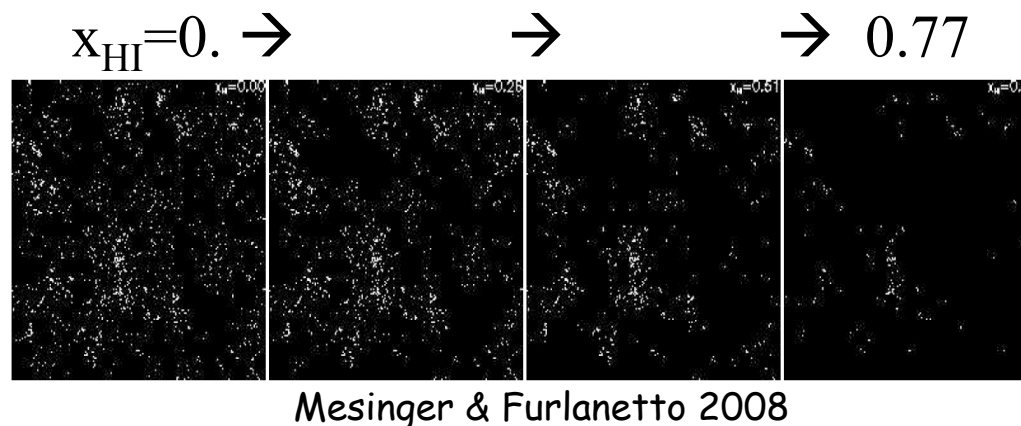
Observational results:

Rapid evolution of the LF for $z > 6$ (e.g., Kashikawa+06, Ouchi+08).

Reionization detected? **NO clear answer**: LF evolution can also be explained by **mass function evolution only** (Dijkstra+07, see also Mesinger & Furlanetto 2008)

Other challenges:

- > these observables also depends on **intrinsic** (unknown so far) properties of the sources (e.g., dust; see Dayal+09).
- > clustering analysis requires **huge** sample (unrealistic for planned near future facilities?).



Constraints (4): CMB polarization

- CMB polarization is generated by electron scattering => the amplitude depends on the Thomson optical depth:

$$\tau(z) = \sigma_T n_{e0} \int_0^z dz' \frac{cdt}{dz'} x_e(z') (1+z')^3$$

which is related to the electron column density:

$$N_e = \tau / \sigma_T = 1.5 \times 10^{23} (\tau / 0.1) \text{ cm}^{-2}$$

Peak position : $l_{peak} \sim 2(s_0 - s_{ri}) / (s_{ri} - s_D) \sim 2(z_r)^{1/2}$

Peak height: $1 - \exp(-\tau_r)$

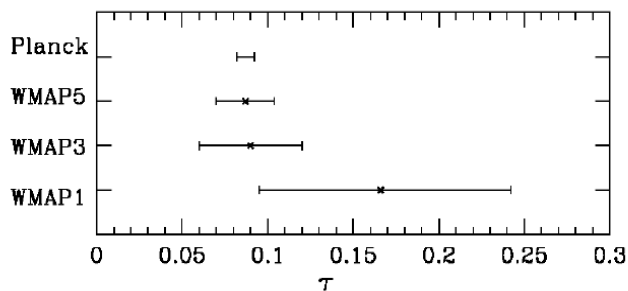
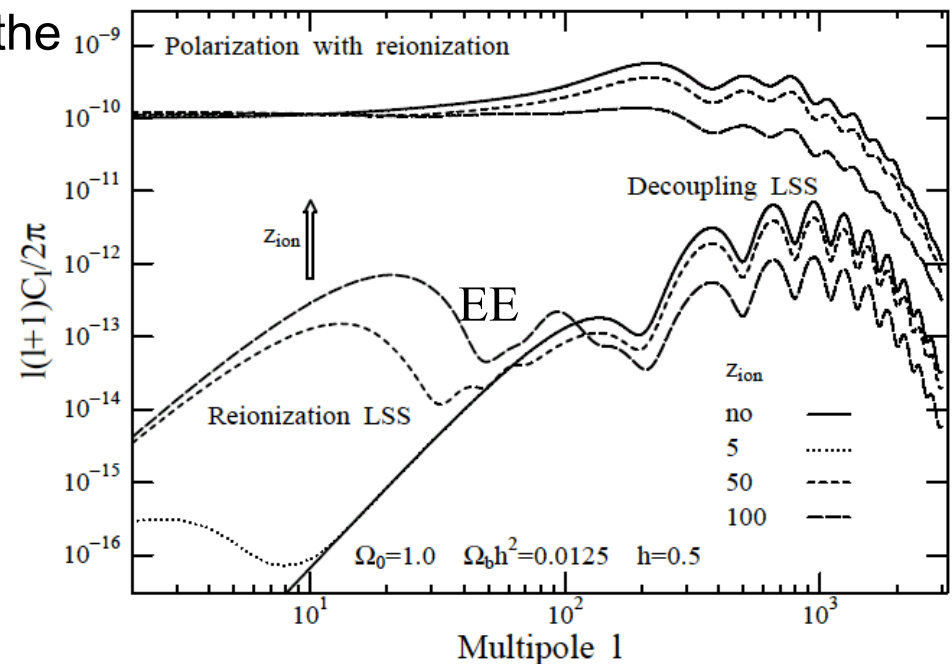
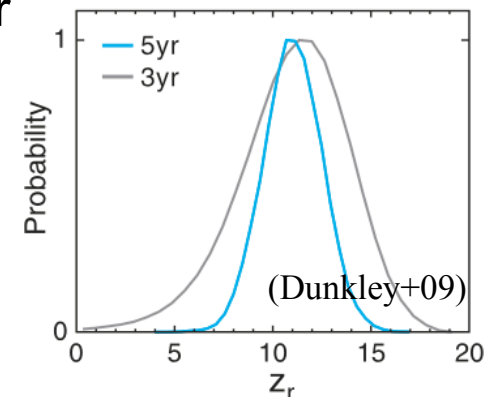


Figure 1. Evolution of WMAP 1 - σ constraints on the optical depth τ_{CMB} and, for comparison, the predicted error for Planck.

BUT: **Integrated value**. To recover z_r we need to “assume” a reionization history.



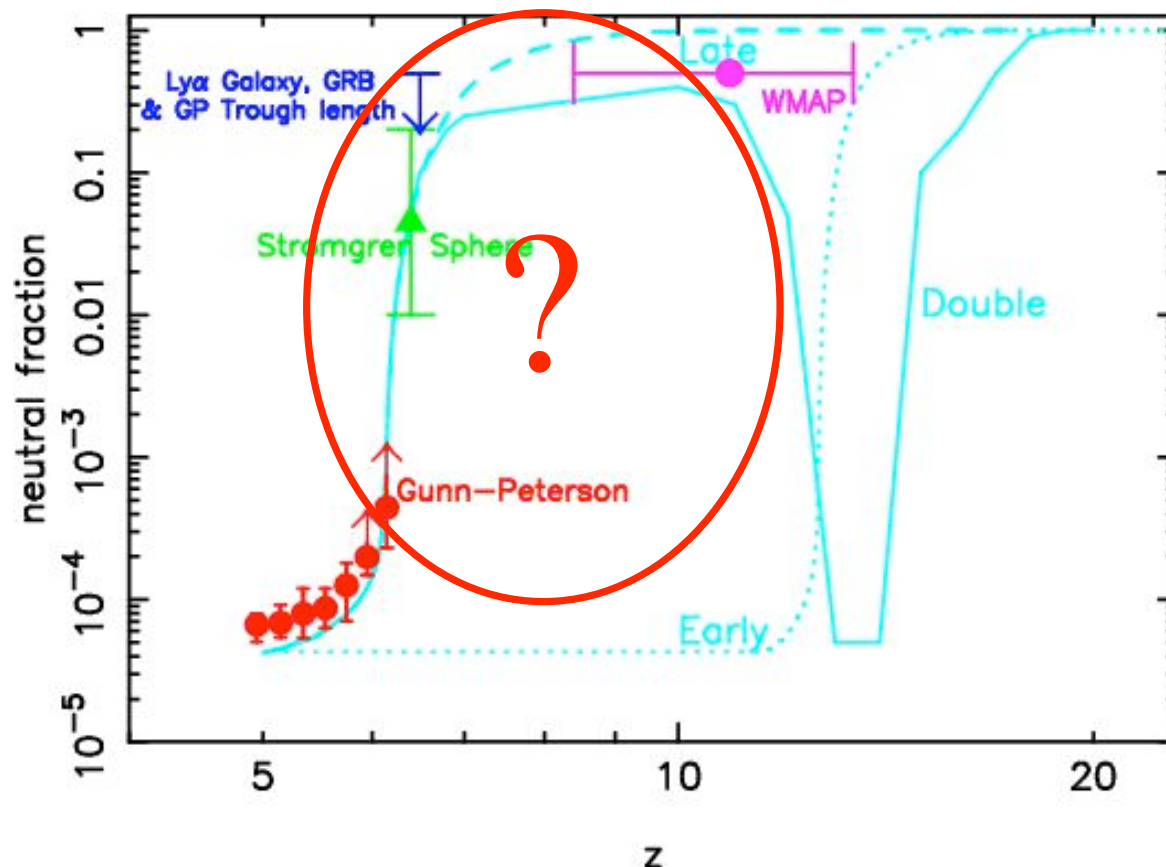
A **partial** list of **other** constraints:

Ly α damping wings,
IGM temperature at $2 < z < 5$,
Gamma-Ray-Bursts,

...

(Mesinger & Haiman 2004, Theun
s+02, Hui & Haiman 2003, Totan
i+06, ...)

Conclusion:
to date, reionization is still
a big **question mark**.



The future is in 21-cm?

expected signal:

$$T_b \approx 23x_{HI}(1+\delta)\left(\frac{1+z}{10}\right)^{1/2}\left(\frac{T_S - T_{bkg}}{T_S}\right) \text{ mK}$$

(at least ~ 4 orders of magnitude smaller than background)

next future: power-spectrum analysis (LOFAR-2010?)

next-next future: direct HI “tomography” (SKA-2020??)

Challenges:

- terrestrial interference
- ionospheric “seeing”
- foregrounds
- instrumental issues

see e.g., Furlanetto+06 and Meiksin 2009 for a review.

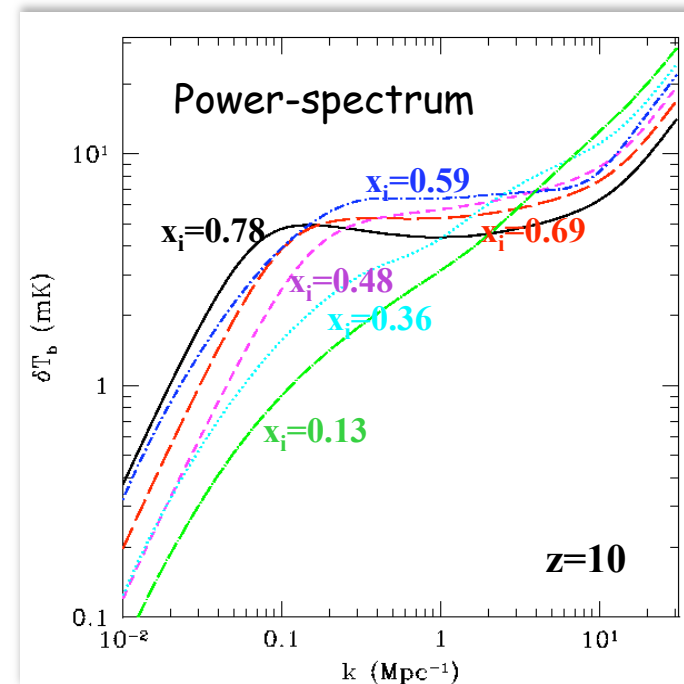
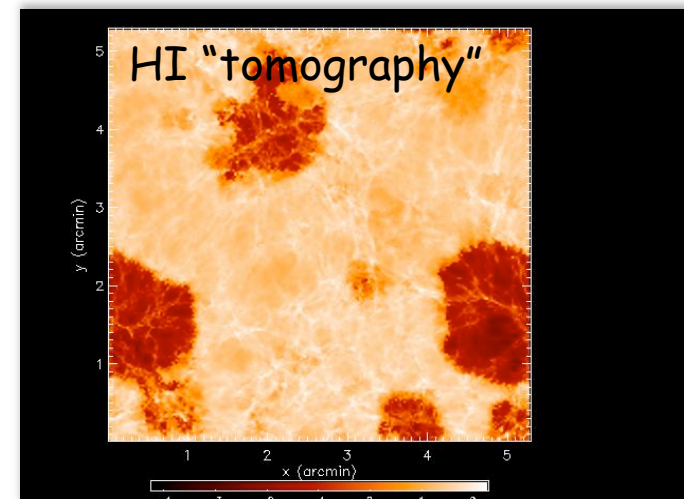
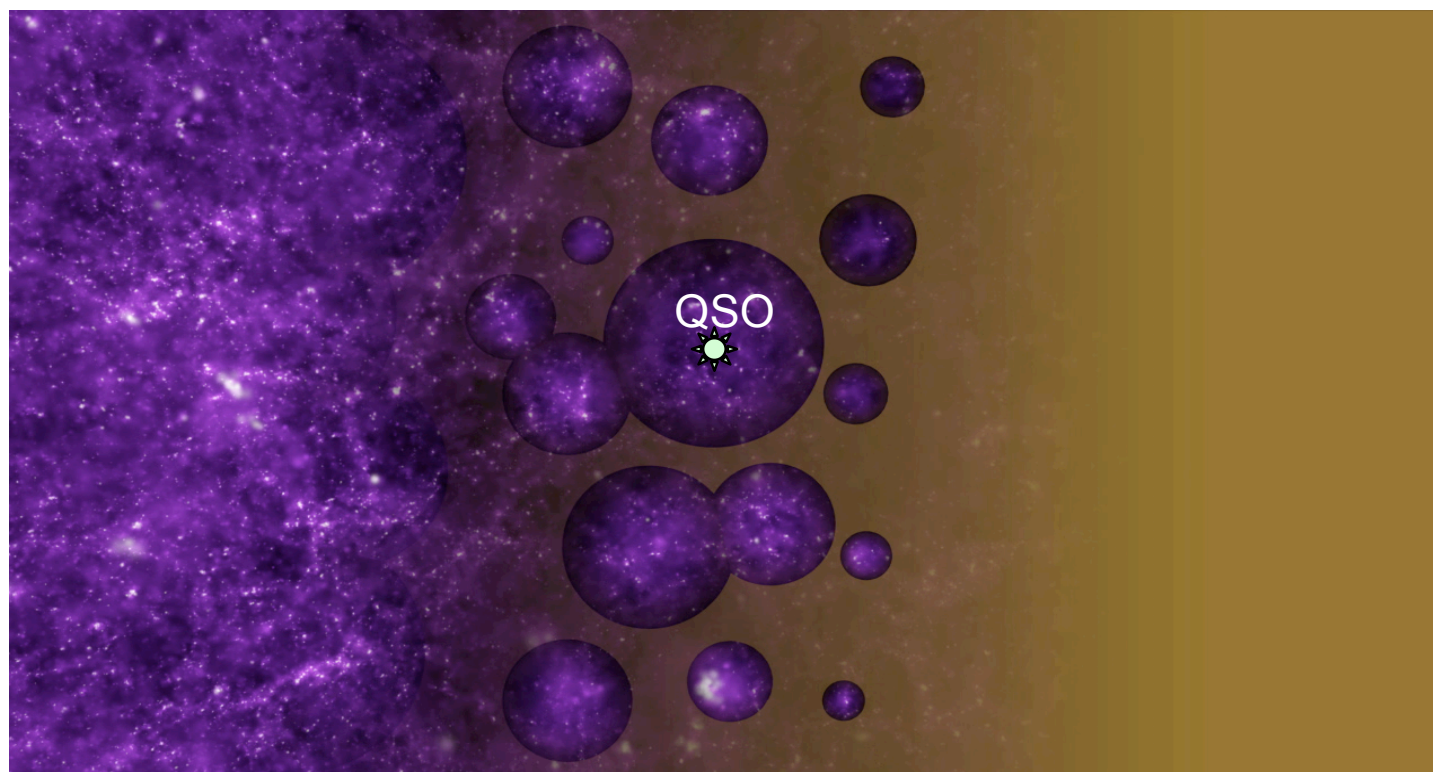


image credits: S. Furlanetto



Alternative (or complementary) approach?

let's try to look the
IGM in *Ly α emission*...



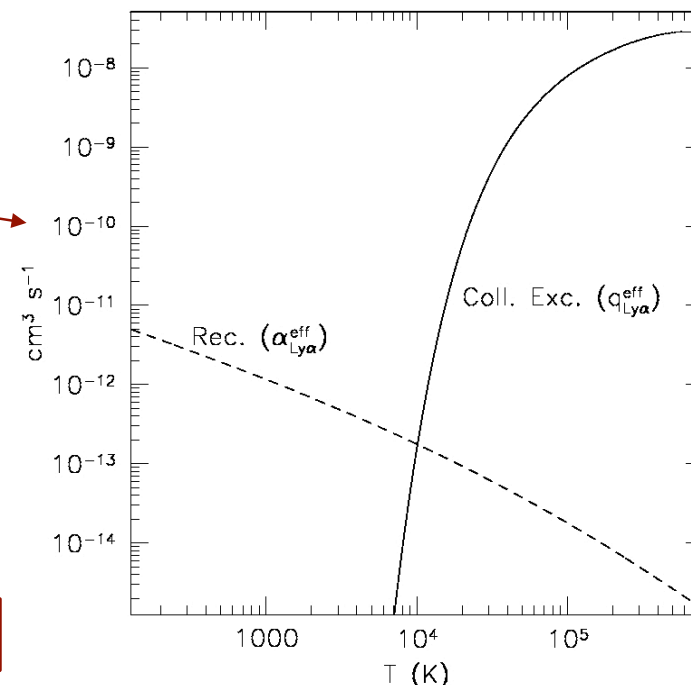
How to map the “bulk” of intergalactic hydrogen during EoR with Ly α emission?

- HII recombination rate is too slow to detect low density gas (Hogan & Weymann 1987; Baltz, Gnedin & Silk 1998).
- Fluorescent emission maps only overdense regions.
- A more efficient mechanism than HII recombination to produce Ly α photons: HI collisional excitation (CE) by energetic electrons.

$$\frac{\text{emissivity}}{h\nu_{\text{Ly}\alpha}} = \text{recombinations } n_e n_p \alpha_{\text{Ly}\alpha}^{\text{eff}}(T) + \text{coll. excitations } n_e n_{\text{HI}} q_{\text{Ly}\alpha}^{\text{eff}}(T)$$

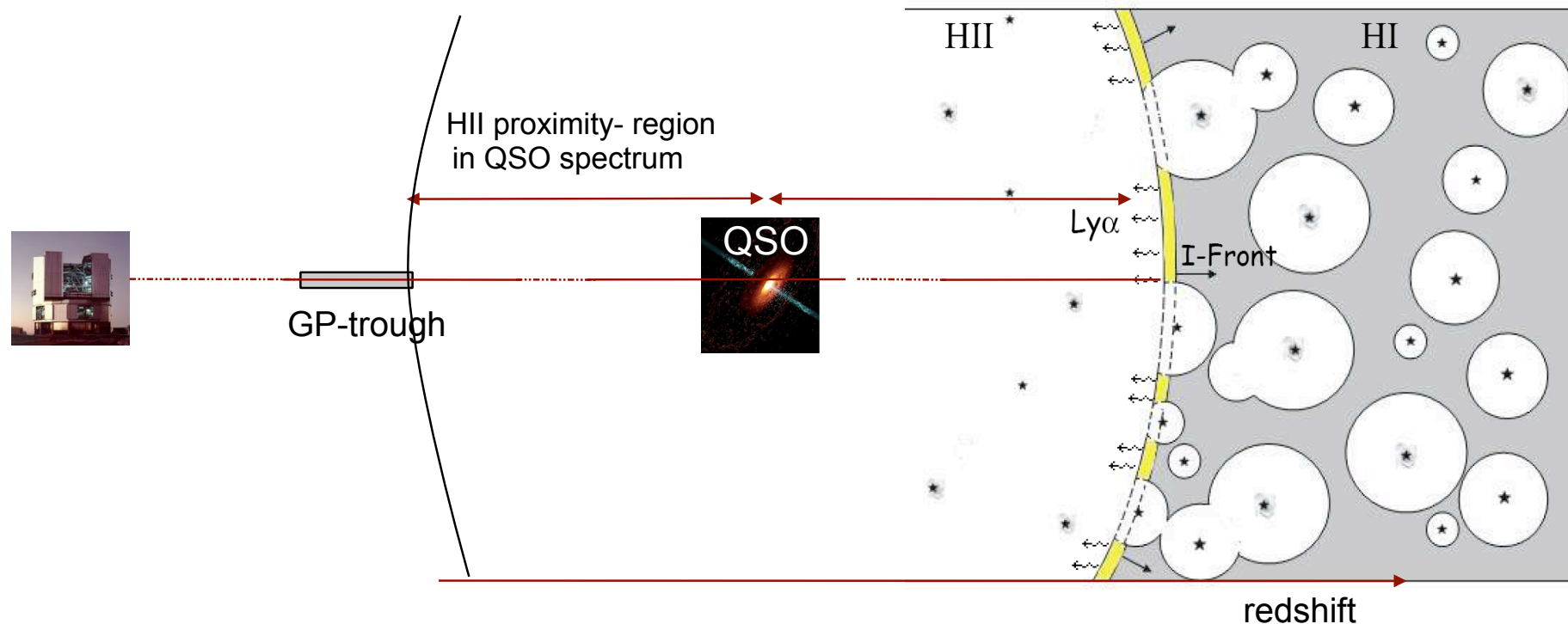
- CE dominates the Ly α emissivity where:
 - neutral fraction (x_{HI}) is ~ 0.5
 - High temperatures: $T > 10^4$ K

→ Typical conditions of QSO Ionization-Fronts



SC, Porciani & Lilly 2008

Mapping HI through the I-Fronts of the highest-z QSOs



→ basic idea:

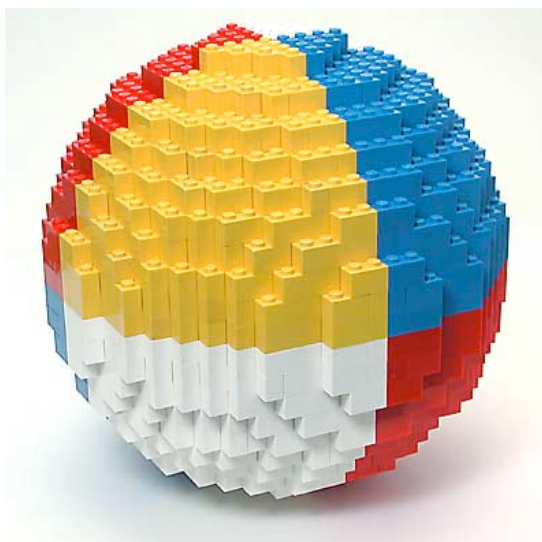
as the I-Front cross the IGM, Ly α photons are produced within the neutral patches via collisional excitations

- The Ly α emission gives a “tomography” of the neutral hydrogen at the I-Front position ($j_{\text{Ly}\alpha} \sim X_{\text{HI}}^2$)
- From the I-Front position we also get:
 - additional information on the average neutral fraction around the QSO
 - constraints on the QSO age and on the emission shape

SC, Porciani & Lilly 2008

OK... but how bright is this signal?

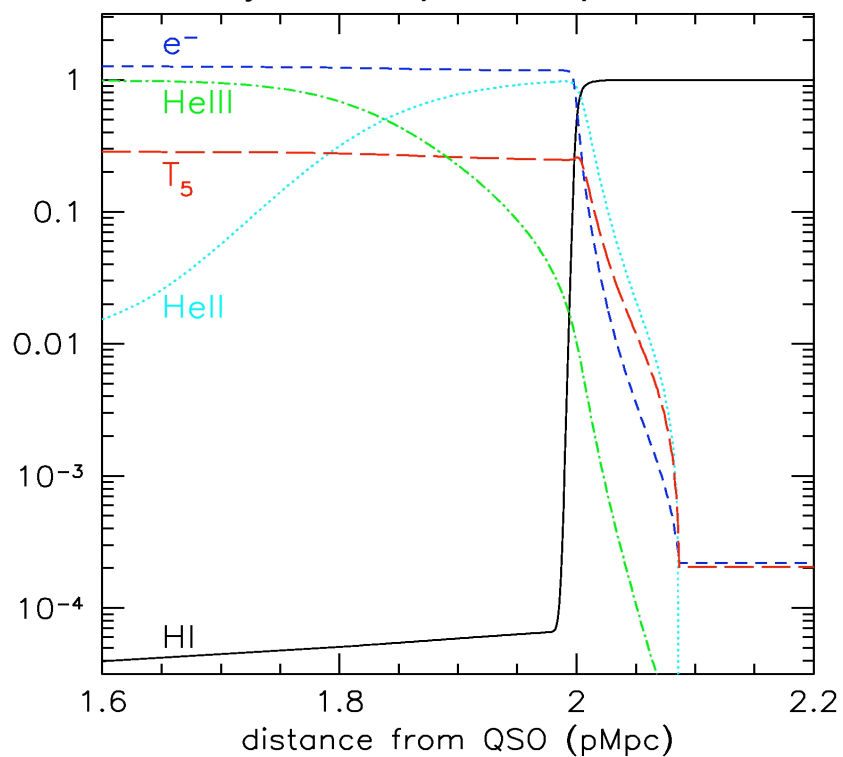
Let's start with a simple spherical model - a QSO surrounded by an uniform IGM - including continuum and Ly α RT (time-dependent, temperature-dependent, Helium, etc.).



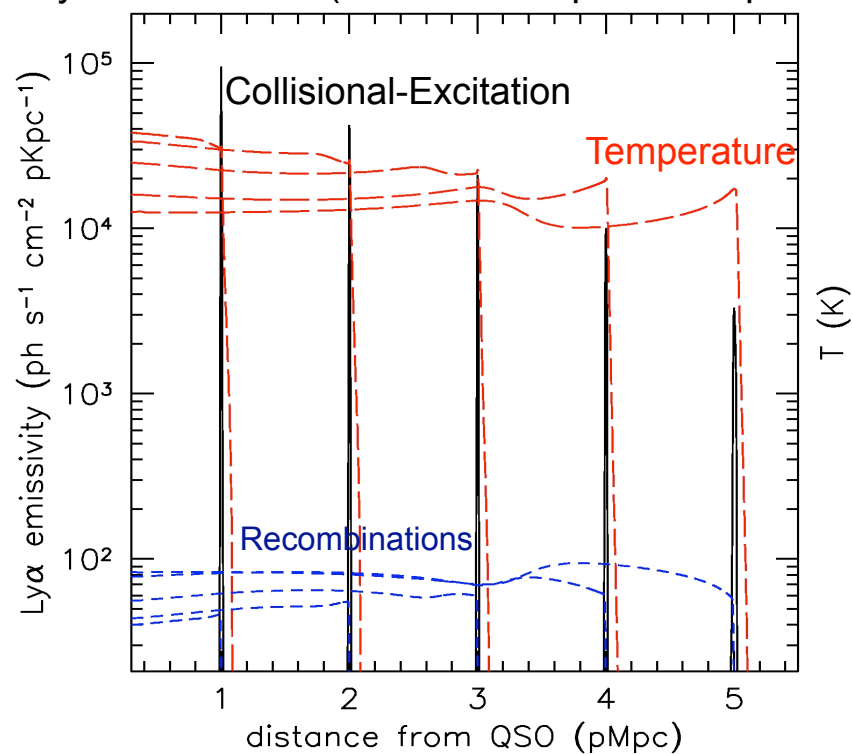
Results: I-front profiles and Ly α emissivity

Example:

I-front density and temperature profiles at $t \sim 10$ Myr



Ly α emissivities (5 different expansion epochs)



• Simulation parameters:

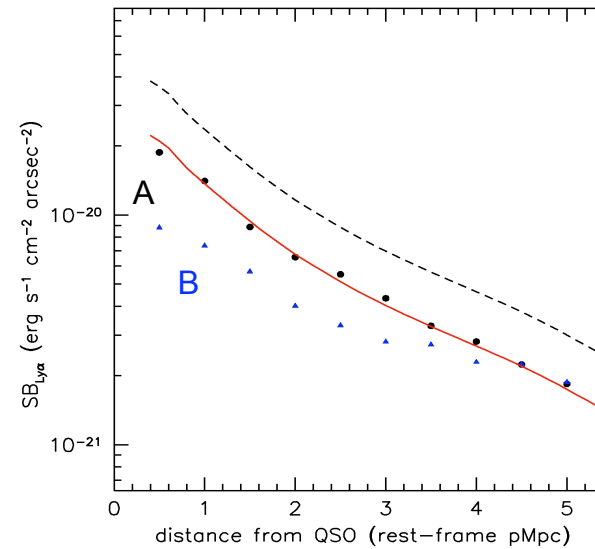
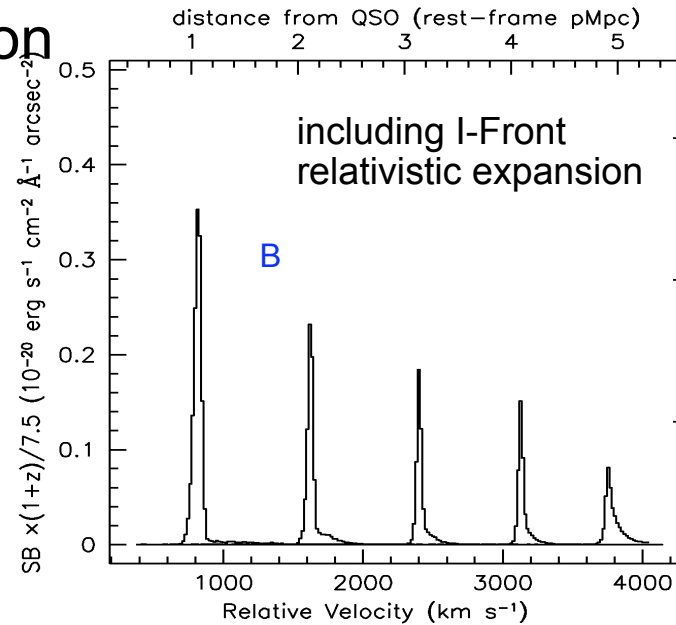
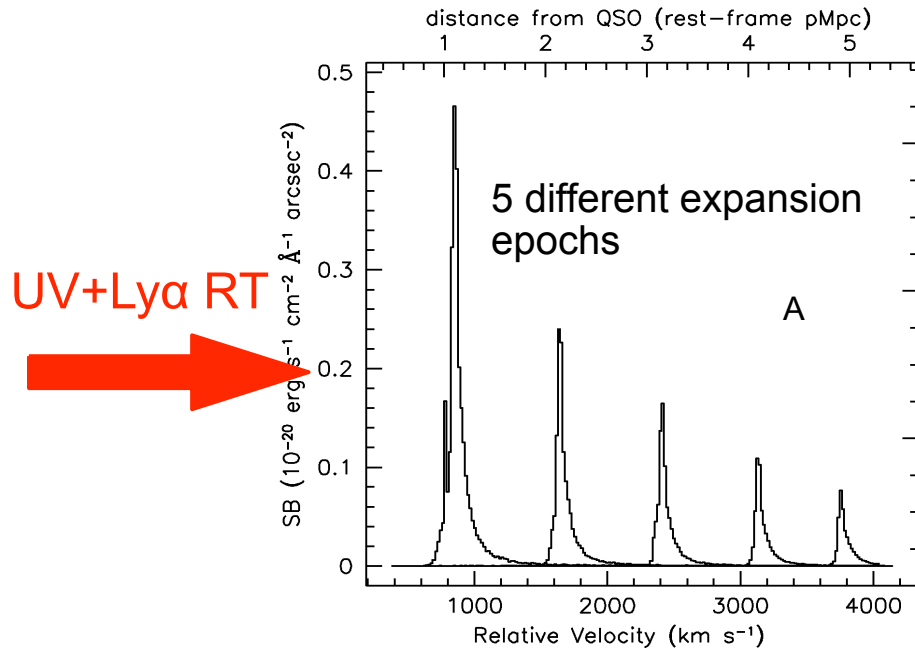
• IGM: $z_{\text{IGM}}=6.5$; $C=35$

$x_{\text{IGM}}=1$; $\delta=0$

• QSO: $N_{\text{ion}}=10^{57} \text{ s}^{-1}$; $\alpha=-1.7$

SC, Porciani & Lilly 2008

Predicted line shape and SB evolution



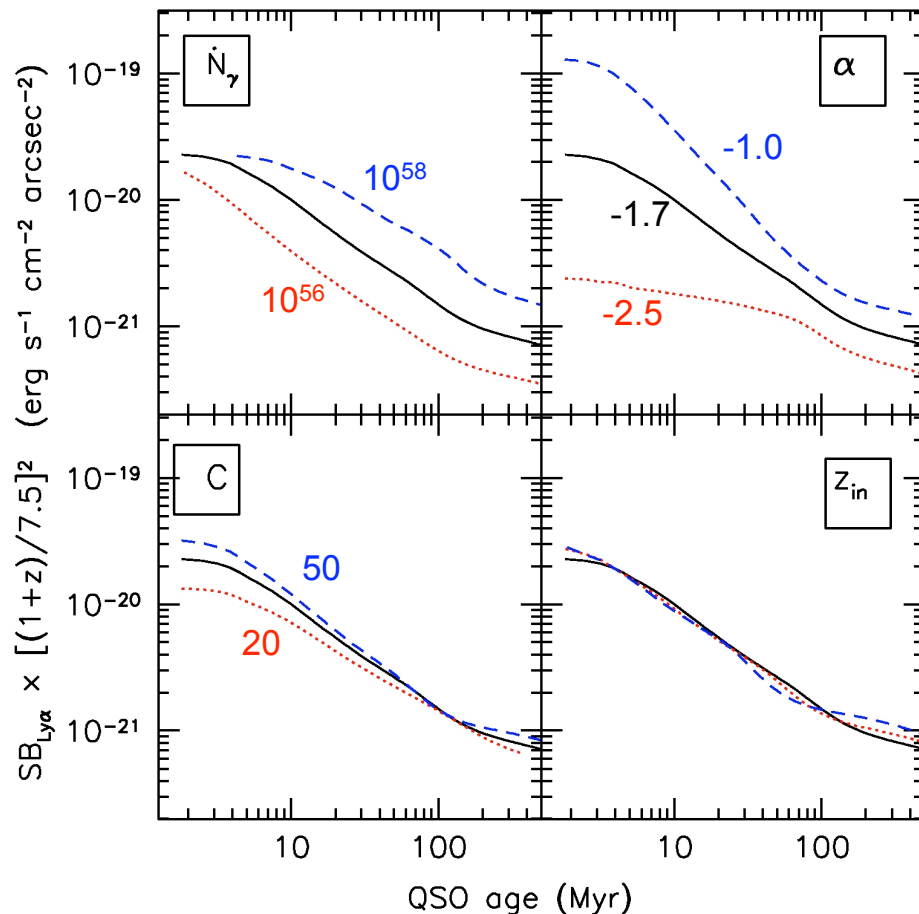
Single line emission (red peak)

Blue peak scattered by residual HI in the QSO bubble.

HI in front of the bubble has a negligible effect on the observed emission.

SC, Porciani & Lilly 2008

Expected Surface Brightness for a large parameter space



Lyα SB from a fully neutral patch of IGM, at mean density, crossed by the I-Front

- $SB_{Ly\alpha} \sim 10^{-20}$ erg/s/cm²/arcsec² for a large range in QSO properties and expected lifetimes

$$SB_{Ly\alpha} \sim 10^{-20} \cdot x_{HI}^2 (1 + \delta)^{1/2} \cdot \left[\frac{t_Q}{10 \text{ Myr}} \right]^{-1} \times \left[\frac{\dot{N}_\gamma}{10^{57} \text{ s}^{-1}} \right]^{1/3} \left[\frac{1+z}{7.5} \right]^{-2} \text{ erg s}^{-1} \text{ cm}^{-2} \text{ arcsec}^{-2}$$

(for $\alpha = -1.7$)

Is it detectable?

- . ~ 3 orders of magnitude below sky-background (better for JWST)
- . but: Line and extended emission (hundreds of arcmin²!)

Possible detection strategy: long-slit (or multi-slit) spectroscopy + integration over the slit length.

- . neutral patch of IGM with few arcminutes scales may be already detected from the ground with current facilities.
- . good redshift dependence, good for (future) $z > 6.5$ QSOs (Pan-STARRS)
with JWST: HI tomography below arcmin scales



But, we should try first to better understand the expected signal...

Towards a **more** realistic modeling: basic **questions**

What is the effect of density **dishomogeneities**?

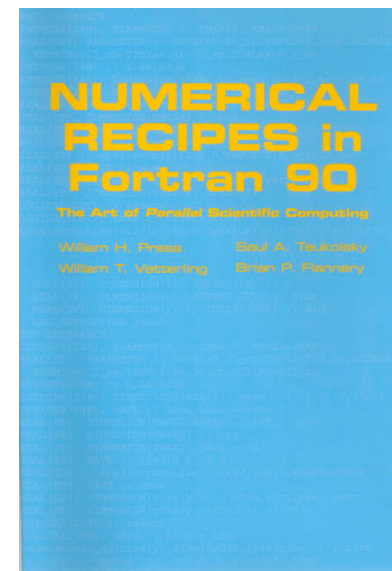
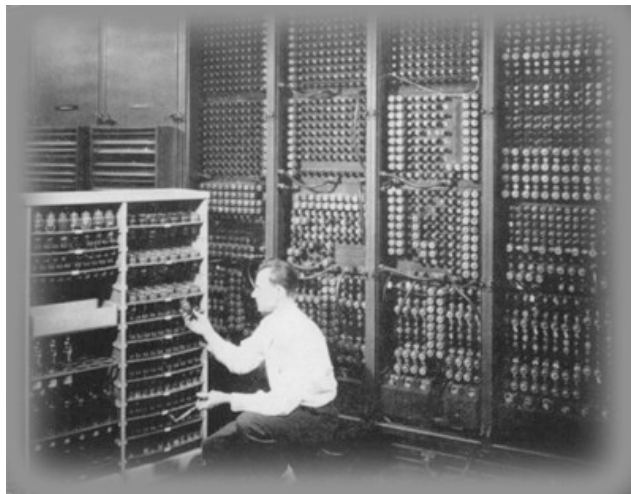
What is the effect of other (galactic) **sources**?

Bright QSO are **rare** objects and should live in **overdense** environment. How does this change the expected signal?

To answer we need: numerical models that follows **large** volumes ($\sim 100\text{Mpc}$) and, at the same time, **resolve the ionization-fronts** ($\sim 10\text{Kpc}$)

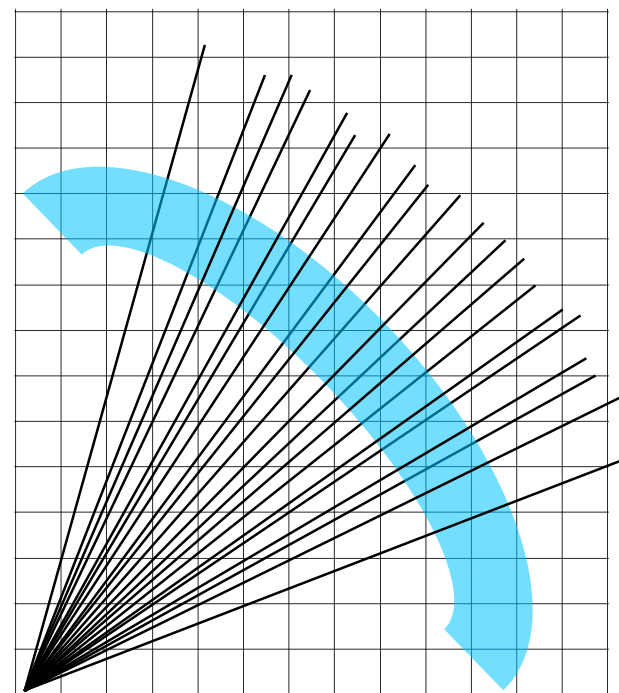
➔ SOLUTION: **Adaptive Mesh Refinement**

“Numerical” digression: building a **new adaptive RT** method for **AMR** simulations



Propagating rays in a grid: “classical” Monte Carlo RT method

- Monte Carlo (MC) sampling of the **solid angle** (uniform rays or Healpix). Photons deposited while rays propagate through the grid.
- Algorithm scales with **angular resolution** (not optimal with multi-meshes; but see also: adaptive ray-splitting).
- Convergence depends on **few** cells (within the I-front), but **all** the cells have to be sampled (solid-angle constraint).

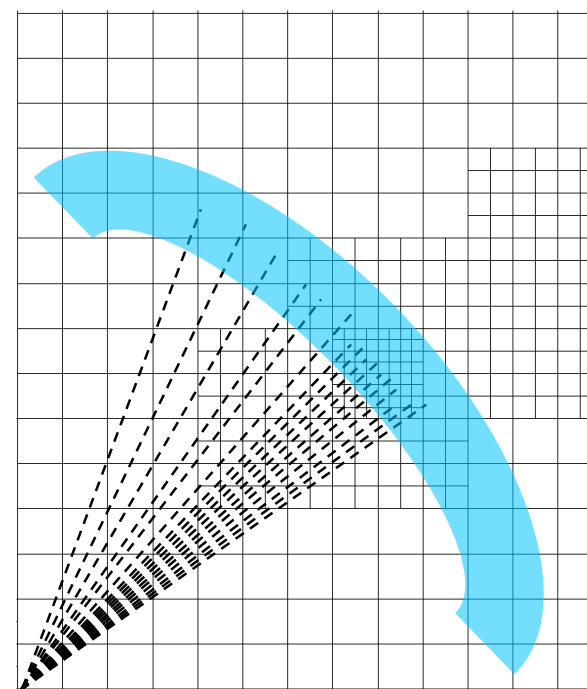


Propagating rays in multi-grids: “RADAMESH”

- Based on a **new algorithm** that tells you:
 - **solid angle** of each cell as seen by any point
 - how to draw rays with correct solid angle distribution **within** each cell

→ **Cell-by-Cell** approach (or cell-by-cell MC)

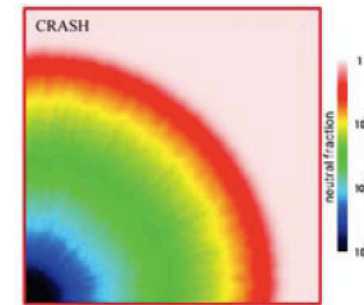
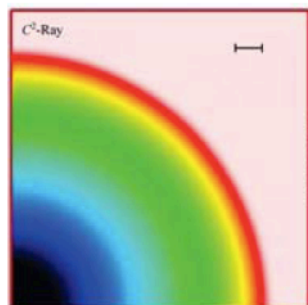
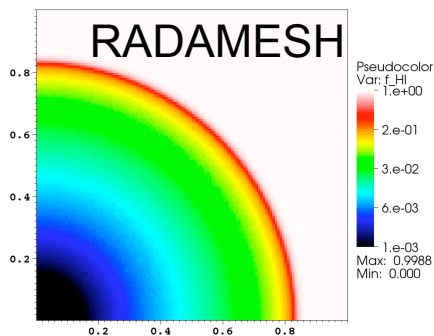
- We are now free to choose the **number of rays** (depositing photons) per cell (e.g., set by **convergence**).
- **Adaptive** to the **physical/grid** properties: efforts concentrate where needed (i.e., for cells within the I-front). It **scales like** $O(N_{\text{front}})$.
- **Adaptive Mesh Refinement on the I-front.**



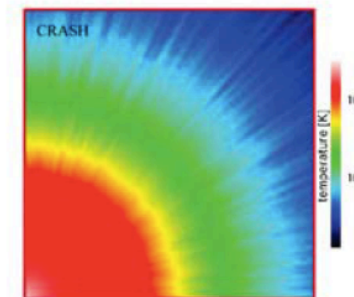
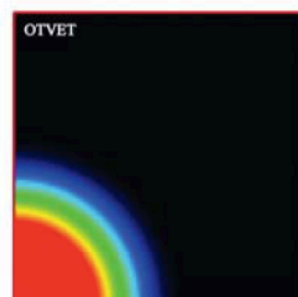
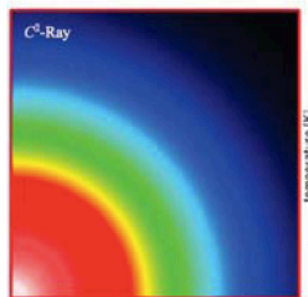
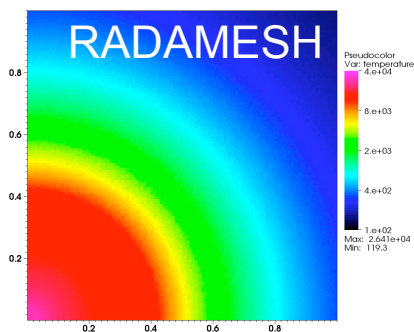
SC & Porciani 2010, in press

from the Code comparison project (Iliev+06):

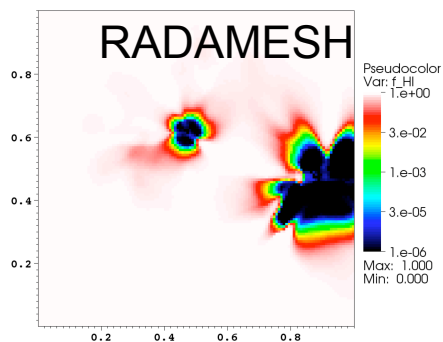
HI fraction



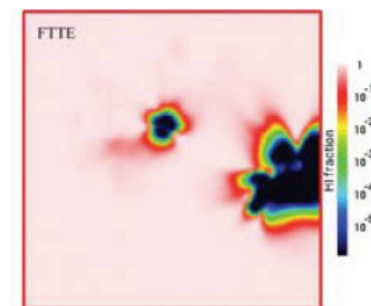
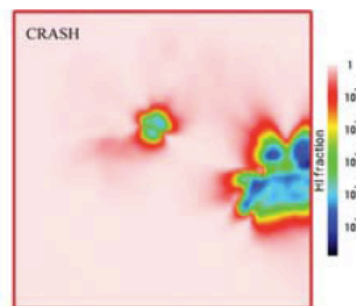
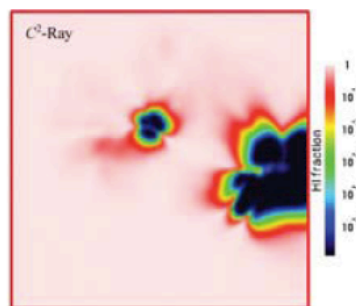
Temperature



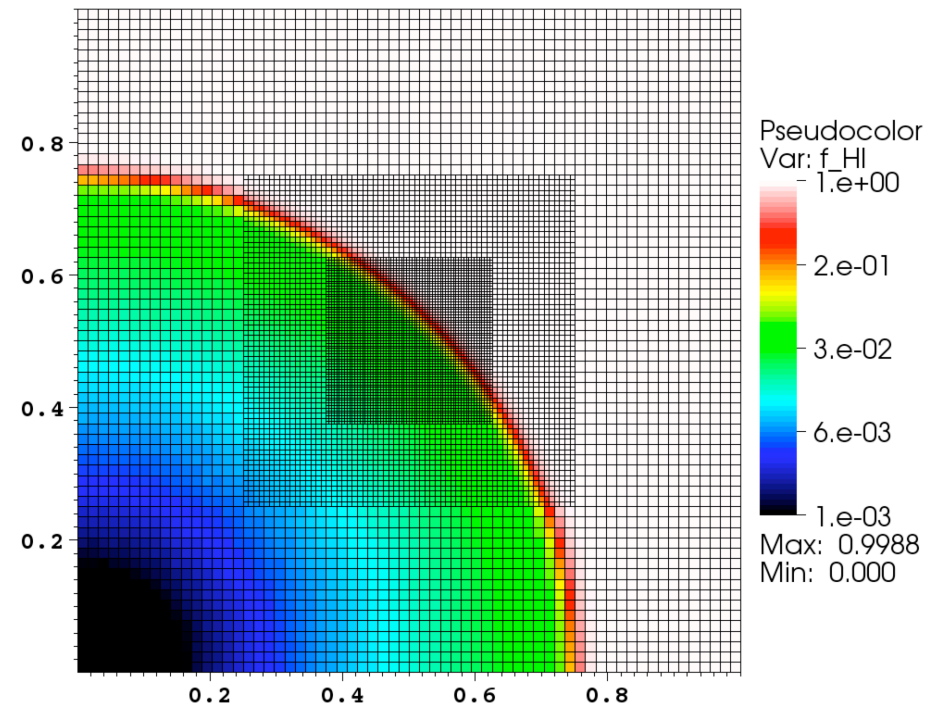
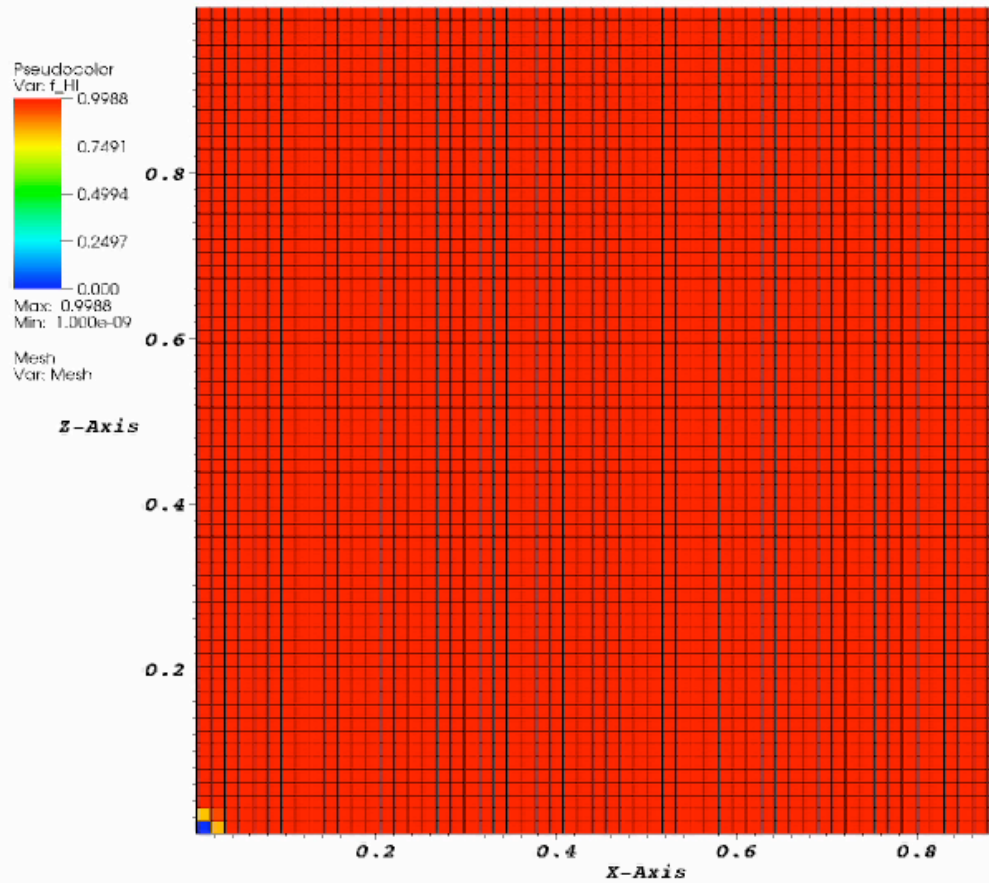
Multi-sources



SC & Porciani 2010



Multi-grids and I-front AMR:



SC & Porciani 2010

We have now the “right” tool...



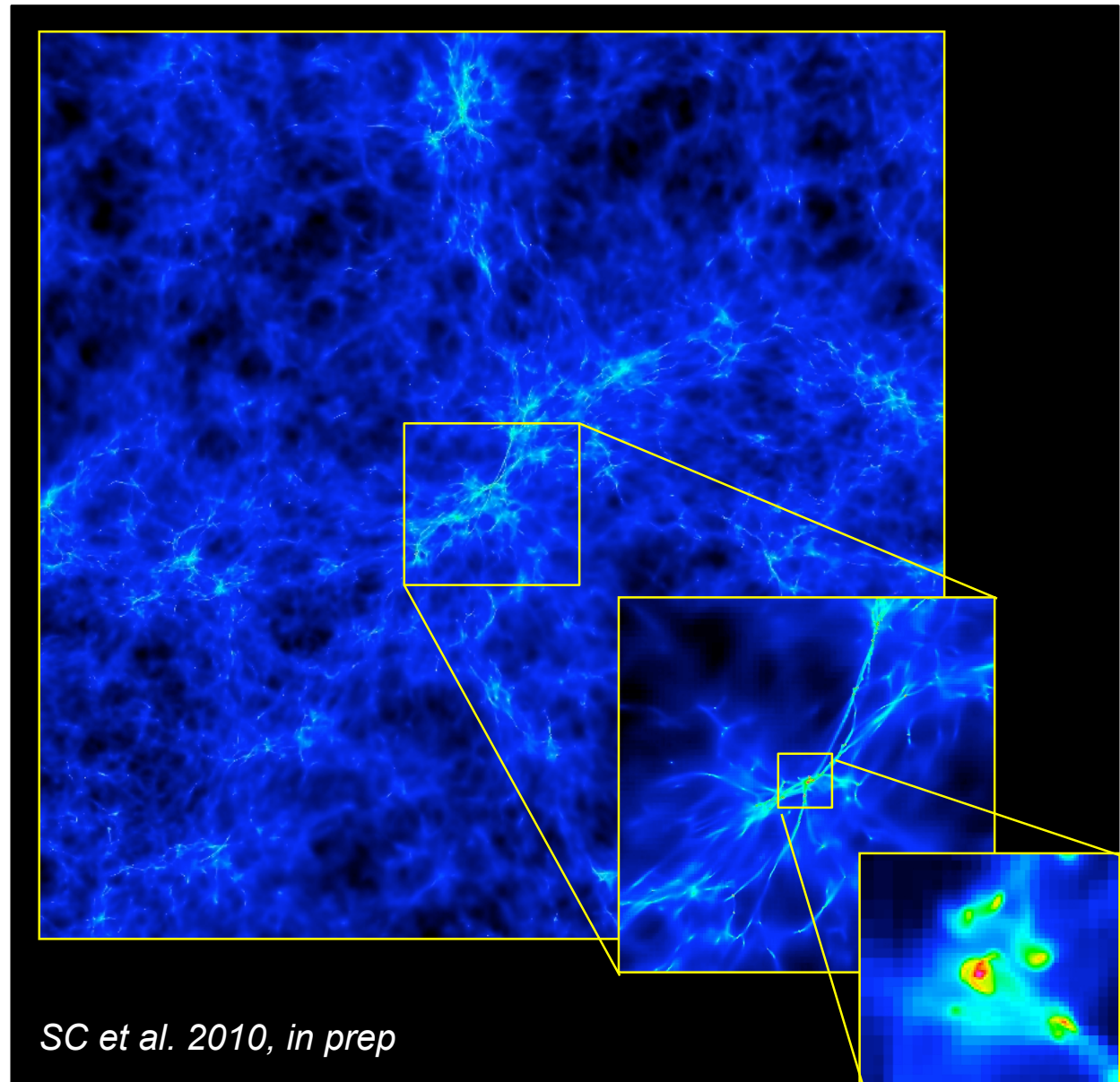
Let's **improve** our previous simple model with the help of **large**, high-resolution **AMR hydro-simulations**

Simulating the **near-zone** of a bright QSO during the EoR

.Series of 200 Mpc zoomed initial condition boxes. **AMR** hydro-runs performed with **RAMSES**.

.Selected halo: $5 \times 10^{12} M_{\odot}$
($z=6.5$)

.High resolution region of **100 Mpc**, 512^3 base grid + 5 levels of refinement (effective physical resolution of ~ 800 pc).



Radiative Transfer Runs: before the QSO turns on

.Performed on an extracted region of size 50 Mpc.

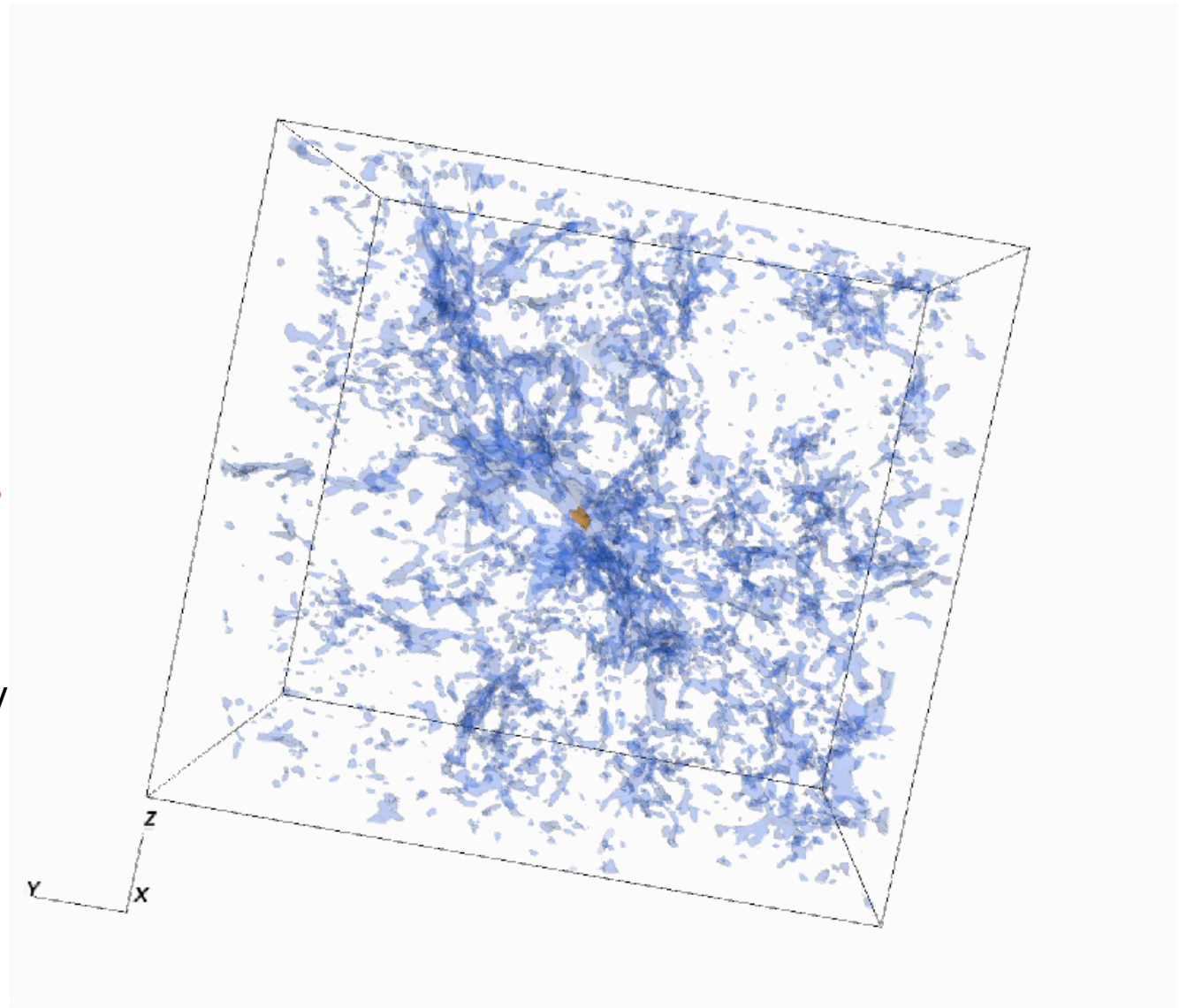
.256³ base grid + 5 levels of refinement (effective physical resolution: ~800pc).

.+ 3 additional levels on I-fronts

.~10⁴ sources (>10⁹ M_⊙), PopII spectrum + QSO.

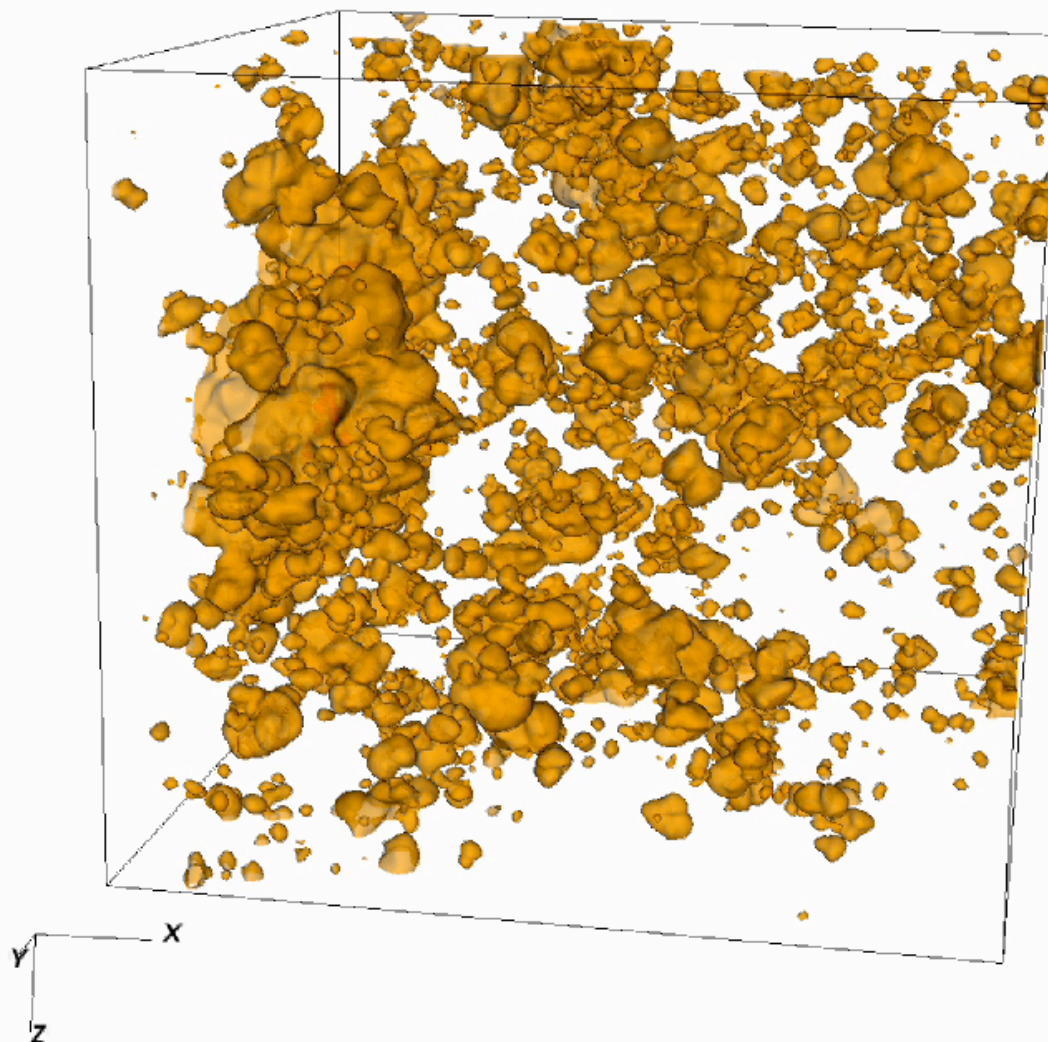
.Including Helium, 70 frequency bins (logarithmically spaced) from 13.6eV to 1keV.

.Including finite light-speed.

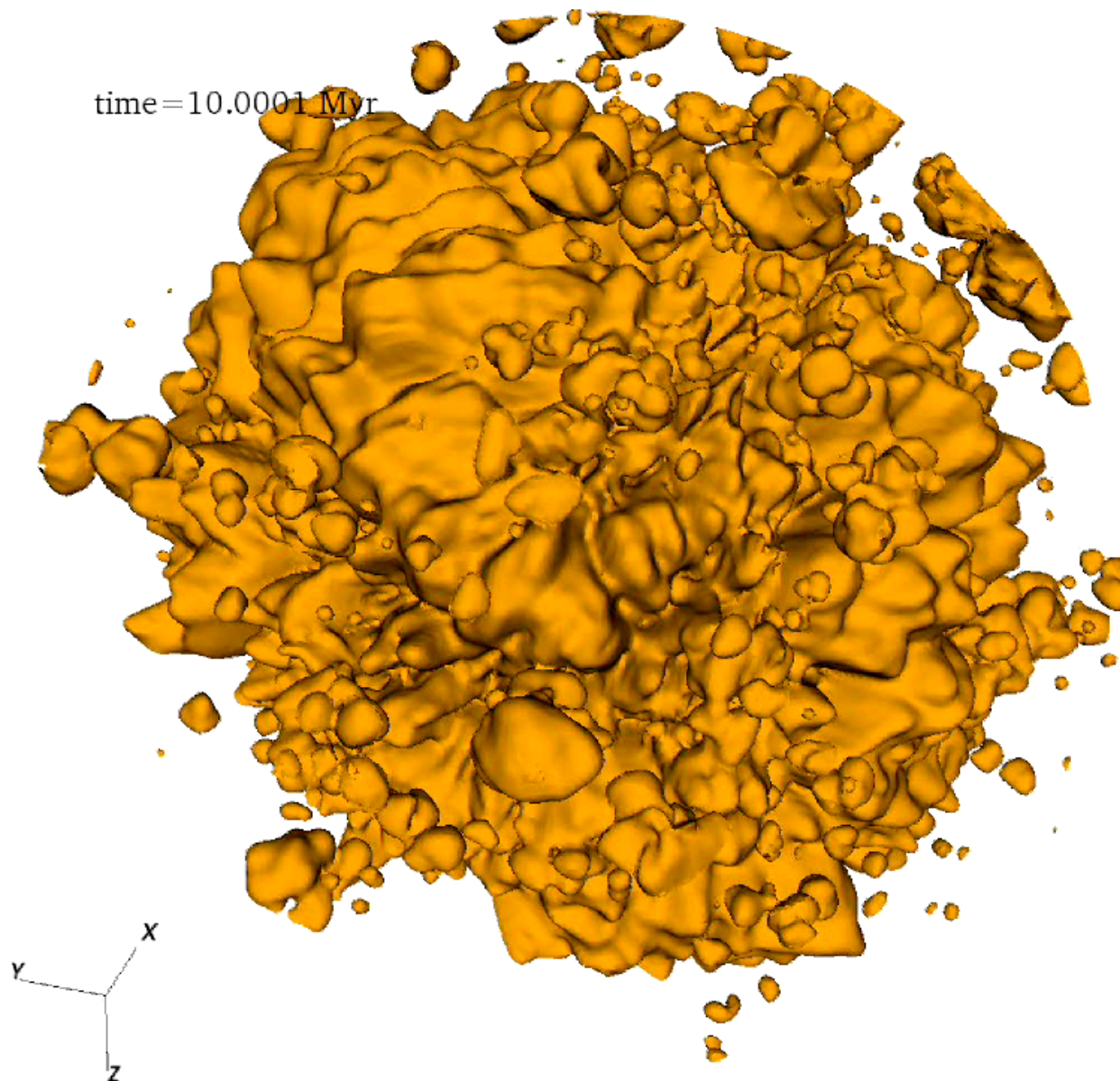


Radiative Transfer Runs: QSO on

time=0.01 Myr

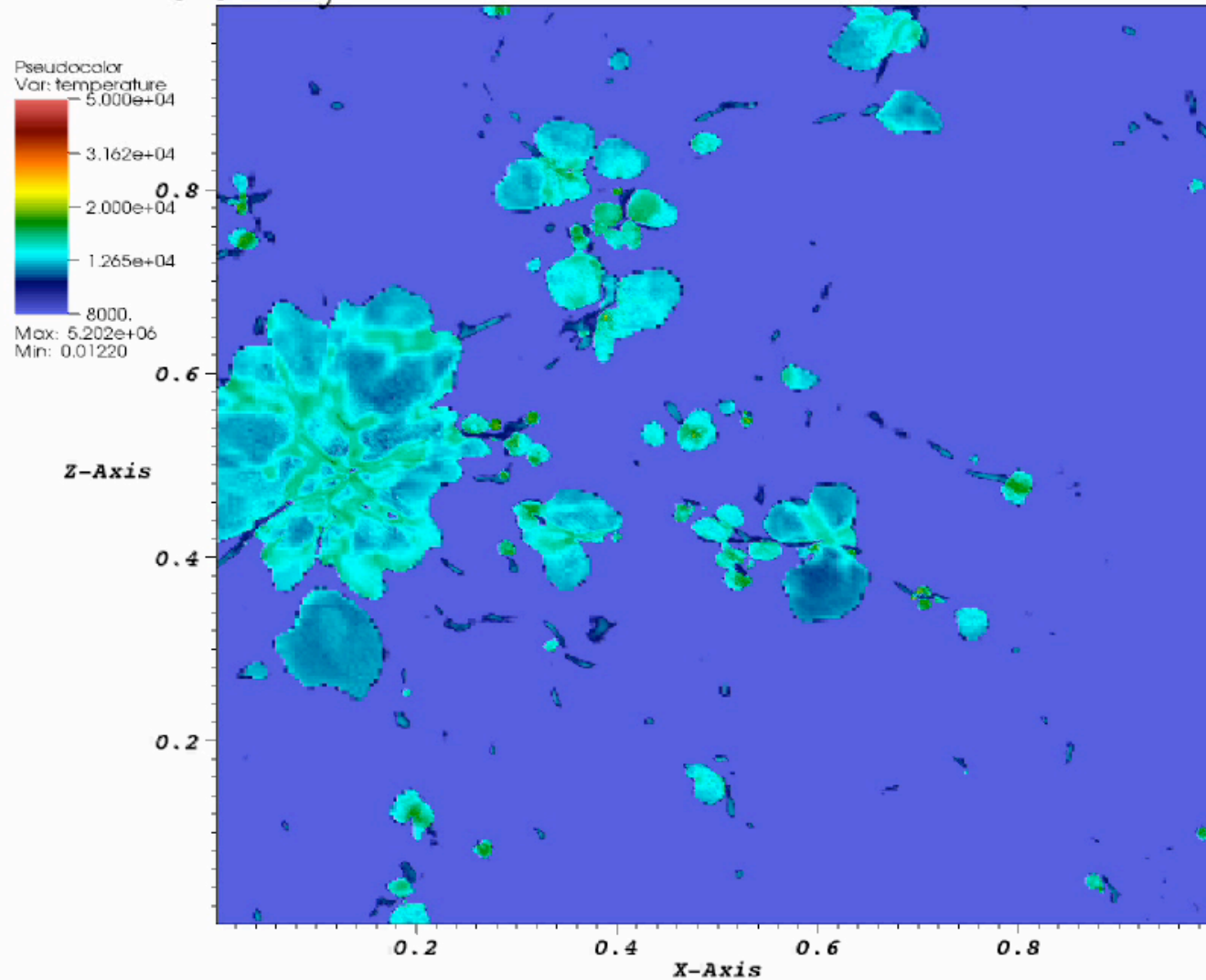


A look inside a QSO bubble



The temperature evolution within the near-zone: a thin slice

time = 0.01 Myr



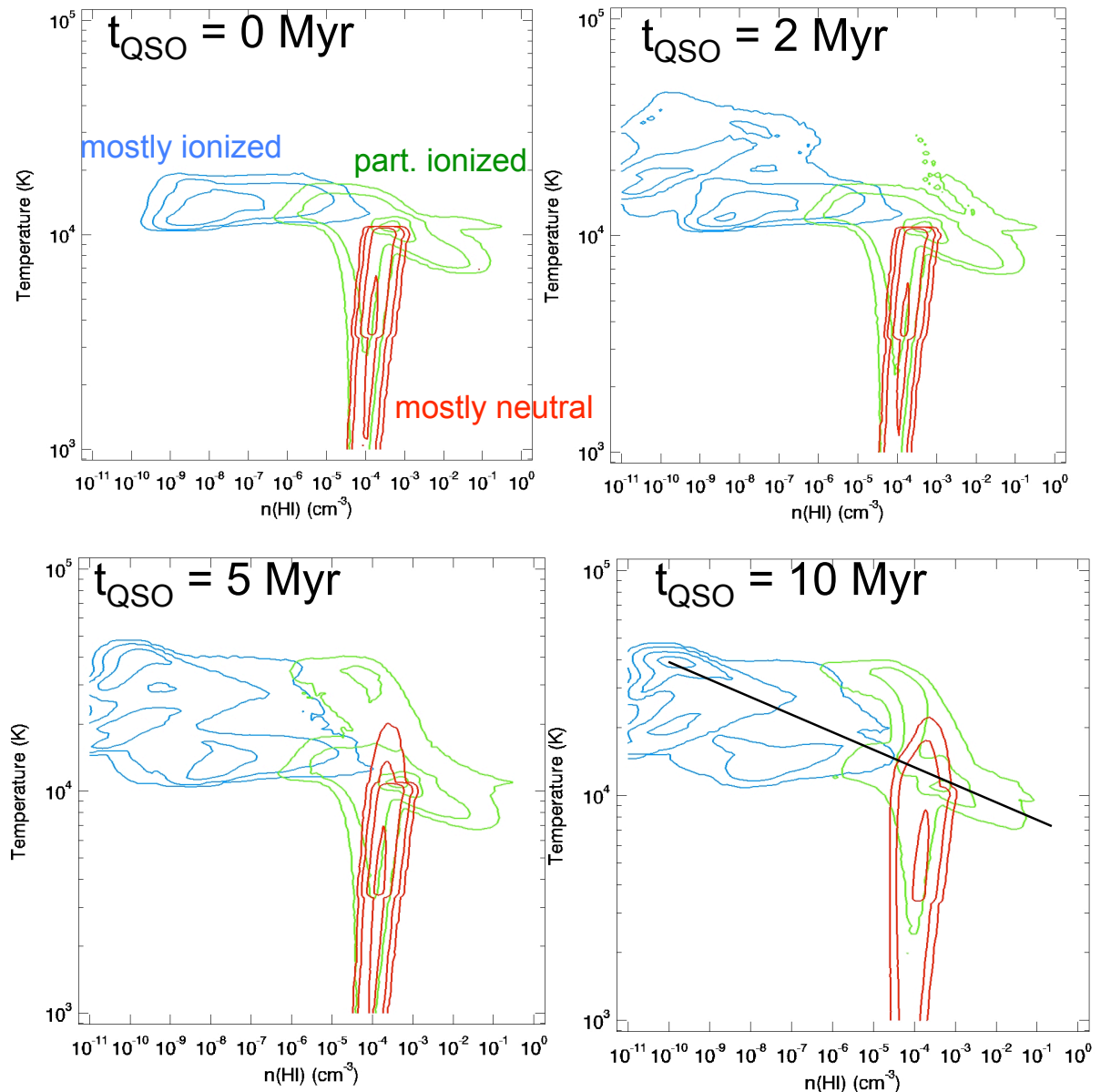
The temperature within the near-zone: phase diagram

As expected (see e.g., Tittley & Meiksin07): bimodal temperature distribution within the qso near-zone:

- Hot regions: H+HeI+HeII ionized by the QSO

- Warm regions: H+HeI ionized by local sources. HeII ionized by the QSO

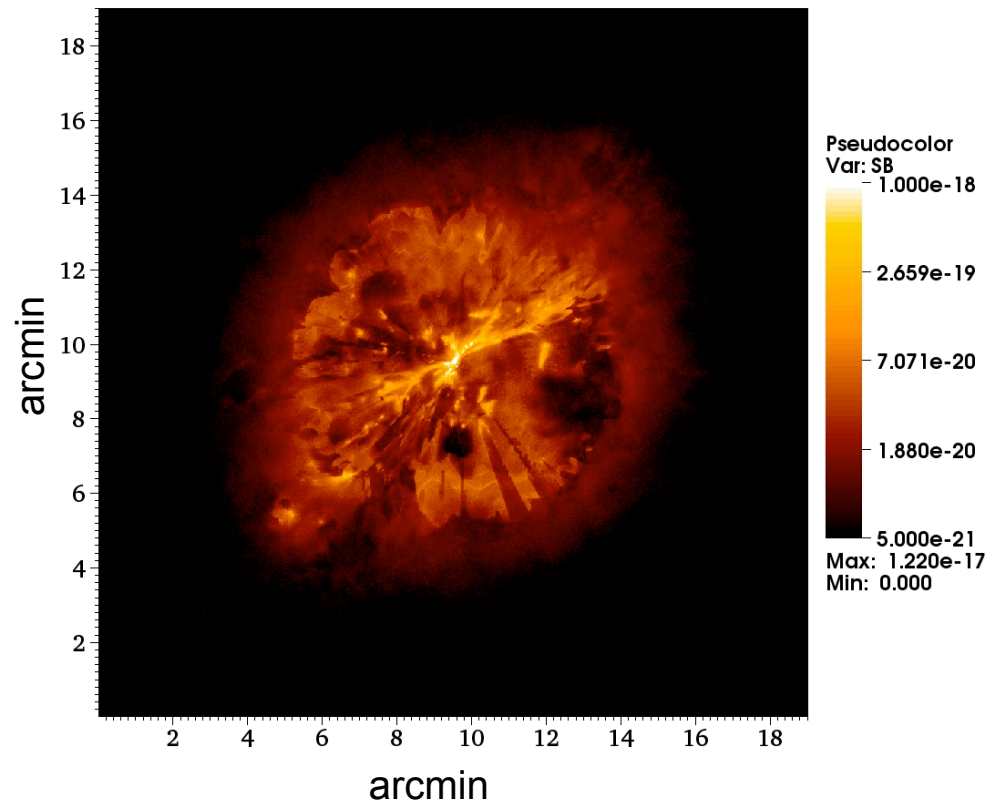
For a given spectrum, overall temperatures are mostly determined by cooling processes within the I-front.



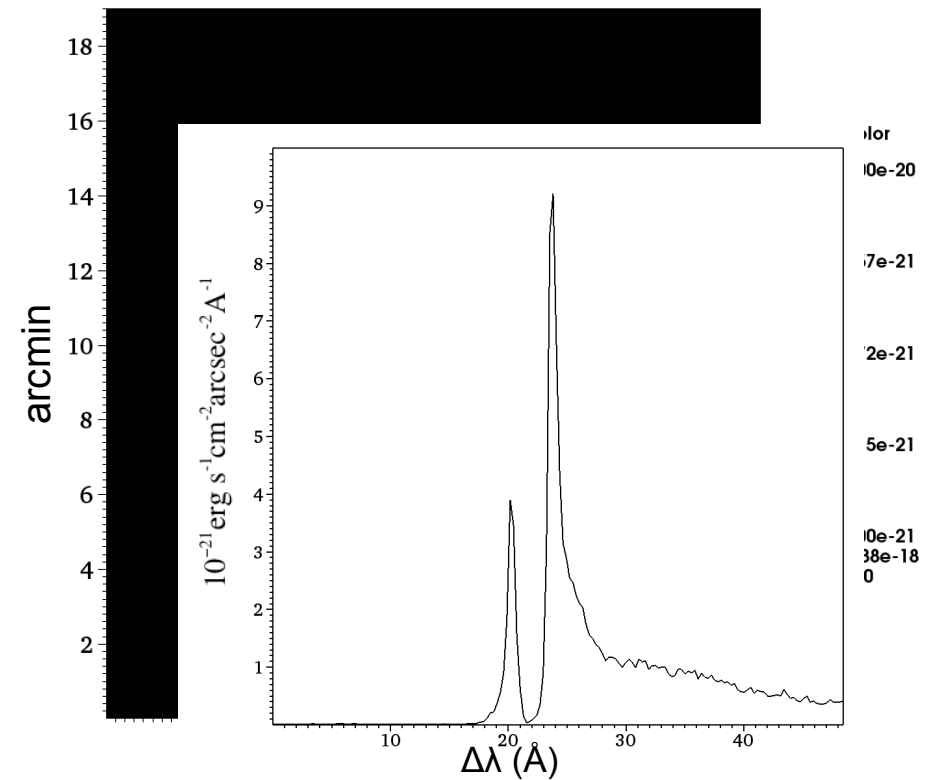
SC et al. 2010, in prep

Ly α RT (preliminary) results:

Narrow Band Image



2D-spectrum



SC et al. 2010, in prep

Summary

- We discussed **Fluorescent Ly α** emission as a way to detect HI **self-shielded clouds** in the high-z IGM before substantial star-formation takes place. We shown theoretical models and first observational results: 13 fluorescent candidates surrounding a bright QSO at $z=3$.
- We presented a **new method** to directly map the HI during **Reionization** through the Ly α emission from QSOs **I-Fronts**.
- Applications:
 - **HI “tomography”** at the emitting I-Front position
 - Constraining the size and shape of **QSO HII regions**
- We calculated the observed properties of this emission simulating the near zone of high-z QSO during the EoR with hydro-simulation and a new adaptive Radiative Transfer code (RADAMESH).
- **Detectability**: neutral (mean density) IGM patches can be detected with current facilities if they extend over few arcmins scales. Otherwise, constraint on the QSO HII region size can be obtained if the mean neutral fraction is greater than 0.1.

BONUS TRACK

Local photo-ionization flux, gas cooling
and galaxy formation

SC, 2010, MNRAS, 403, L16

Evolution of the observed Star Formation Rates (SFR)

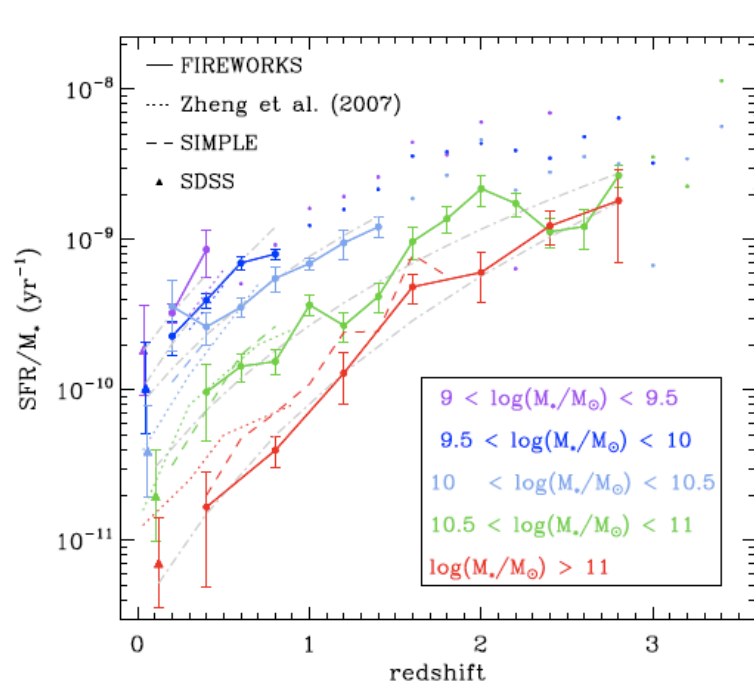


Figure 2. sSFR vs. redshift in different mass bins. Filled, connected circles are the FIREWORKS results, dots show where mass incompleteness starts to play a role. The error bars represent bootstrap errors. The dashed and dotted lines represent results from Damen et al. (2009) and Zheng et al. (2007), respectively. SDSS data were used to include a local data point (triangles). Linear fits to the FIREWORKS results are displayed using gray dash-dotted lines. The fits show that the SSFR increases with z at a rate that appears independent of mass.

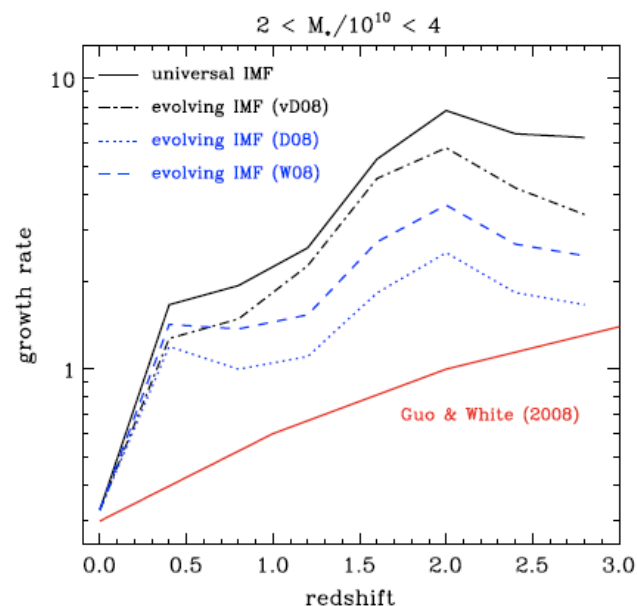


Figure 5. Dimensionless growth rate as a function of redshift for galaxies with masses ranging from $2 \times 10^{10} M_{\odot}$ to $4 \times 10^{10} M_{\odot}$. The black solid line shows the FIREWORKS result when a Kroupa (2001) IMF is applied. The dash-dotted lines, dashed, and dotted lines show the FIREWORKS growth rate based on an evolving IMF, according to the parameterization of van Dokkum (2008, vD08), Davé (2008, D08), and Wilkins et al. (2008, W08), respectively. The corrected values based on the IMFs of D08 and W08 (in blue) are lower limits, since they do not include the effect an evolving IMF has on the stellar mass. Introducing a time-dependent IMF decreases the discrepancy between the observations and the simulated results from Guo & White (2008; red solid line), but it does not completely resolve it. In particular, the steep increase in observed growth rate at low redshift ($z = 0-1$) is still evident.

Damen et al. 2009

How to obtain the steep decline at low z ?

Two possibilities: 1) remove the gas from the galaxy (SN feedback)
2) reduce/stop cooling gas accretion from halo

Solution (1): requires to fix unconstrained physical parameters (winds, mass loading factor, etc.) and fine tuning. Not able to explain a large range of observations (e.g., $s\text{SFR}-M_*$, see Bouche'+10).

Solution (2): cooling gas accretion is governed by “simple” atomic physics, ions abundances and gas temperature.

➡ basic idea (Efstathiou 1992): every process that is able to change cooling ions abundances is able to change cooling gas accretion.
e.g., UV background suppresses H+He cooling and thus the formation of low mass haloes with $T_{\text{vir}} < \text{few times } 10^4 \text{ K}$.

What about a “local” photo-ionization background and the cooling in more massive haloes (also due to metal cooling)?

The observed relation between Star Formation activity and Soft X-ray emission: some examples

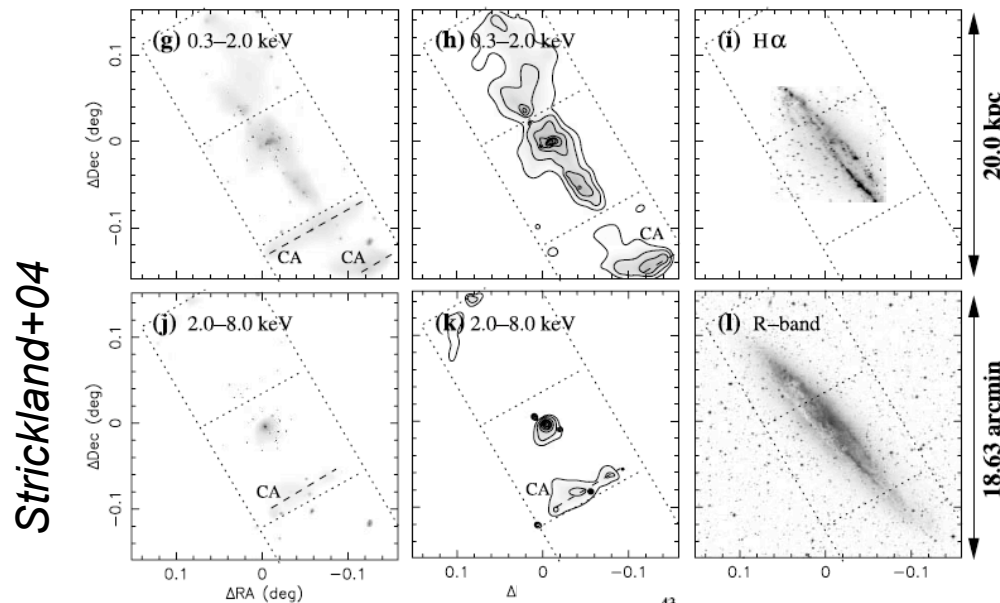
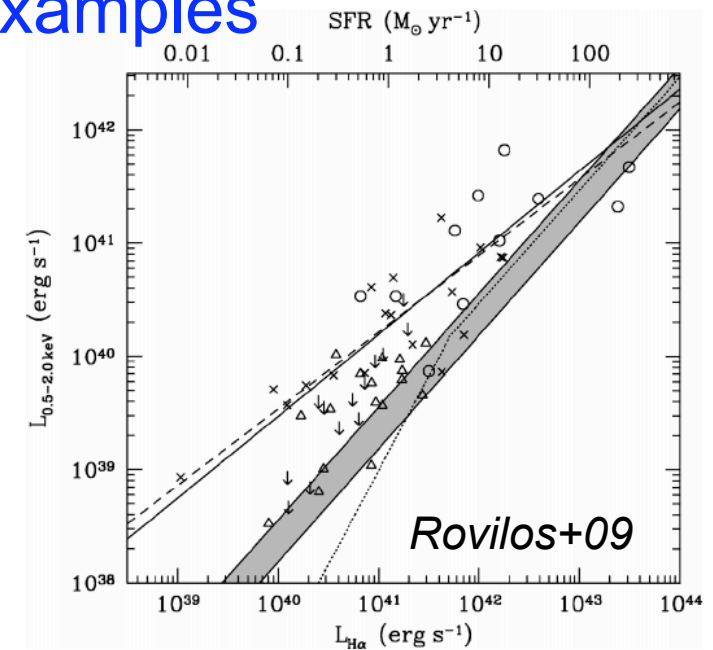


Fig. 9.—*Chandra* X-ray and optical images of NGC 4945. The meaning of CA is described in Fig. 2.



Mas-Hesse+07

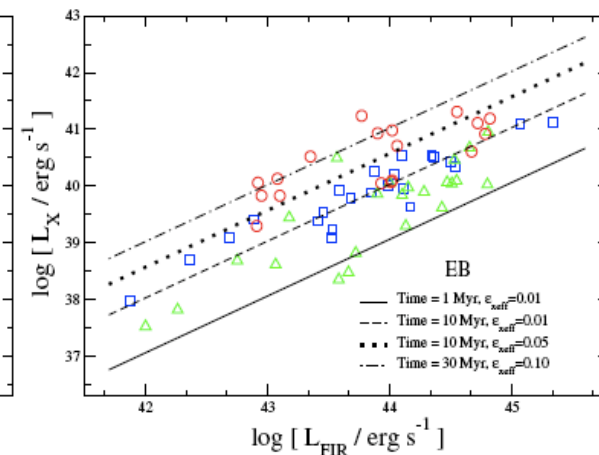
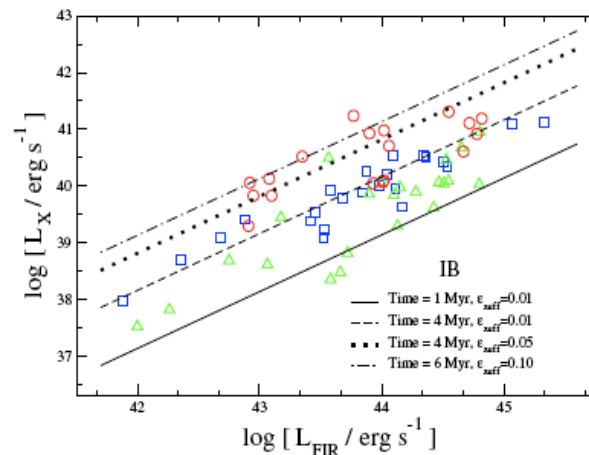
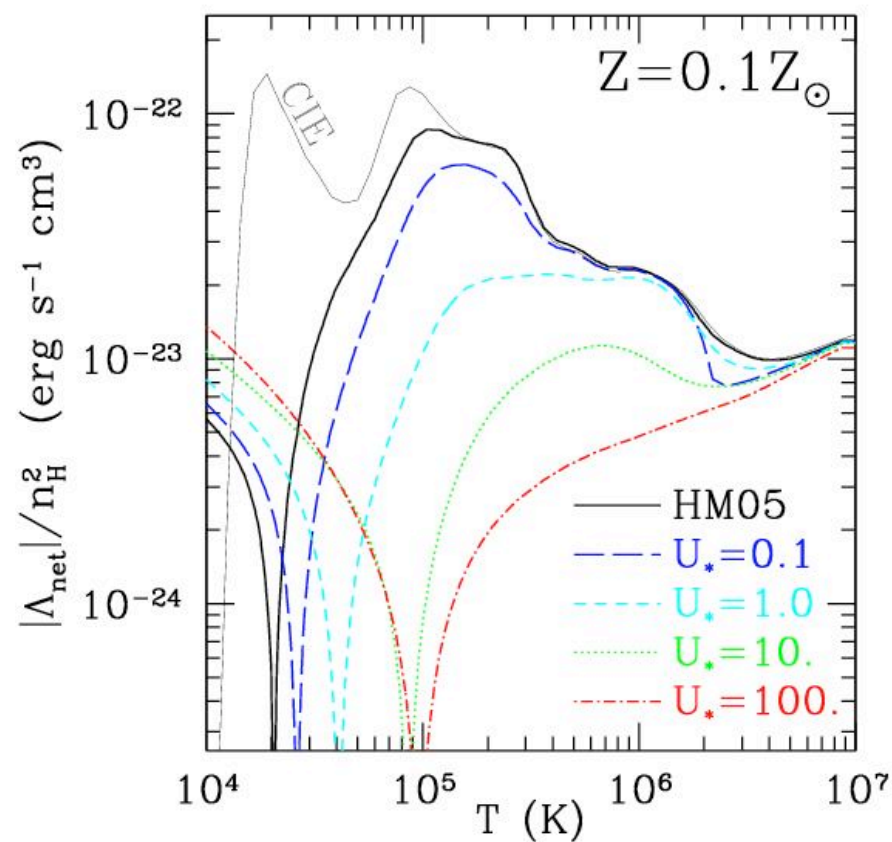
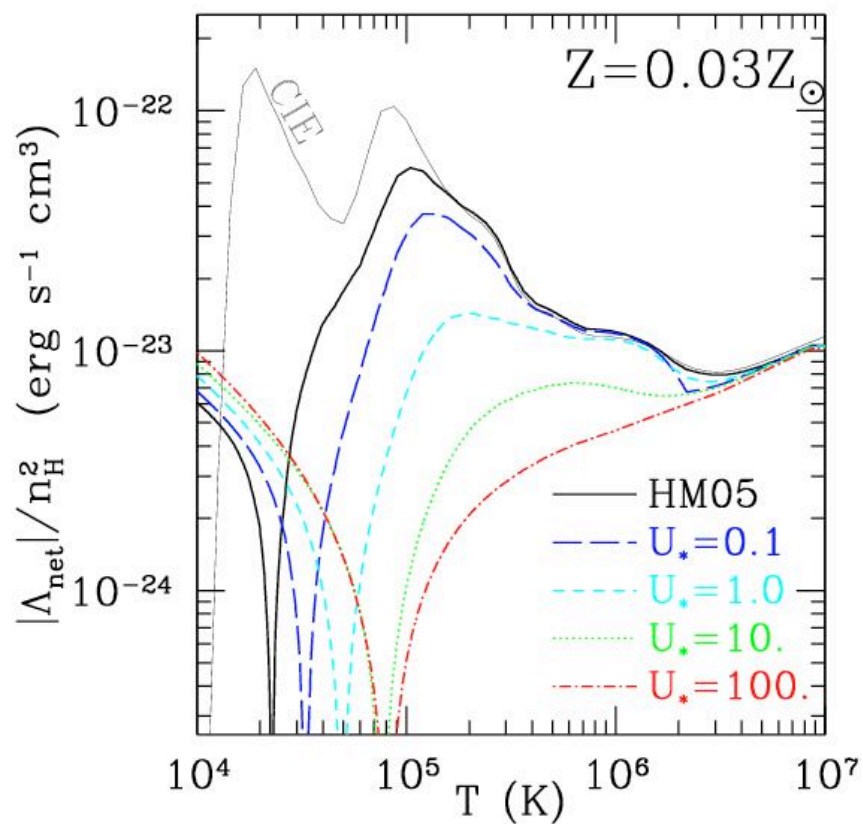


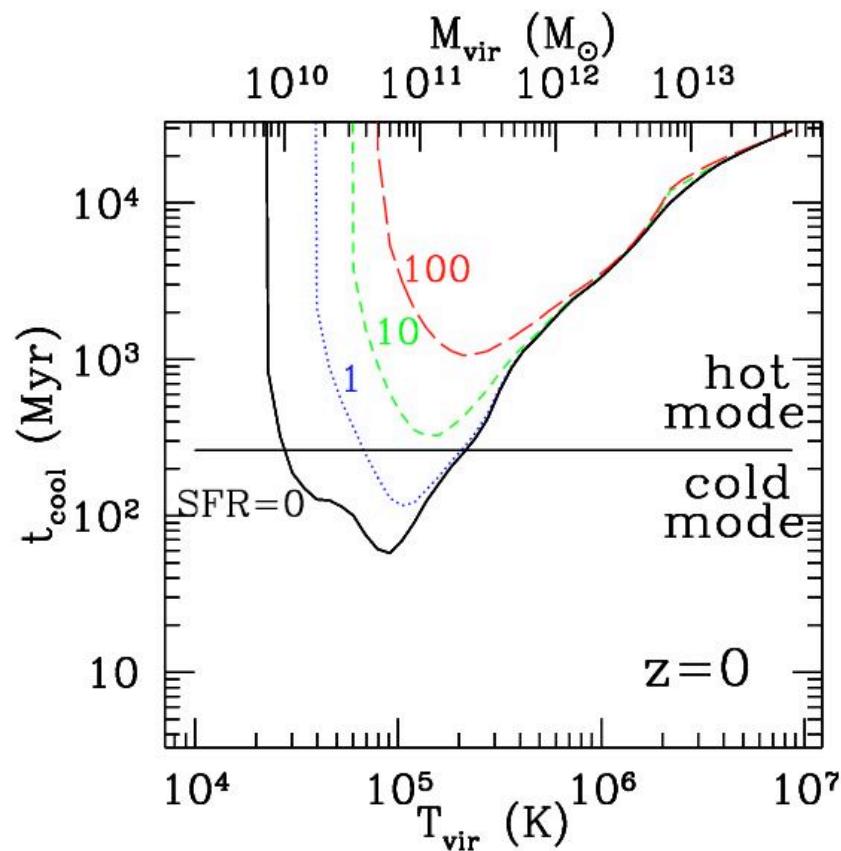
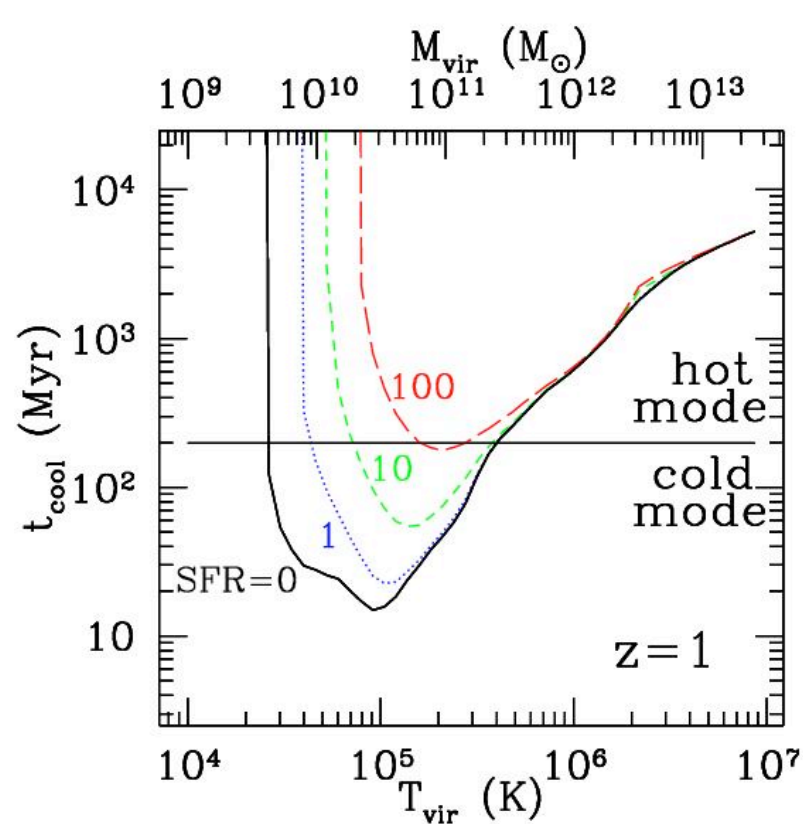
Fig. 6. L_{softX} vs. L_{FIR} for the RCS03 (squares), TUL06 (triangles) and ROSA07 (circles) samples. In the left panel we have overplotted the correlation lines corresponding to the $L_{\text{softX}}/L_{\text{FIR}}$ ratios predicted by IB models for different ages and ϵ_{eff} values. The right panel shows the corresponding predictions for EB models.

Effect on the Cooling rate of circum-galactic gas (CLOUDY models)



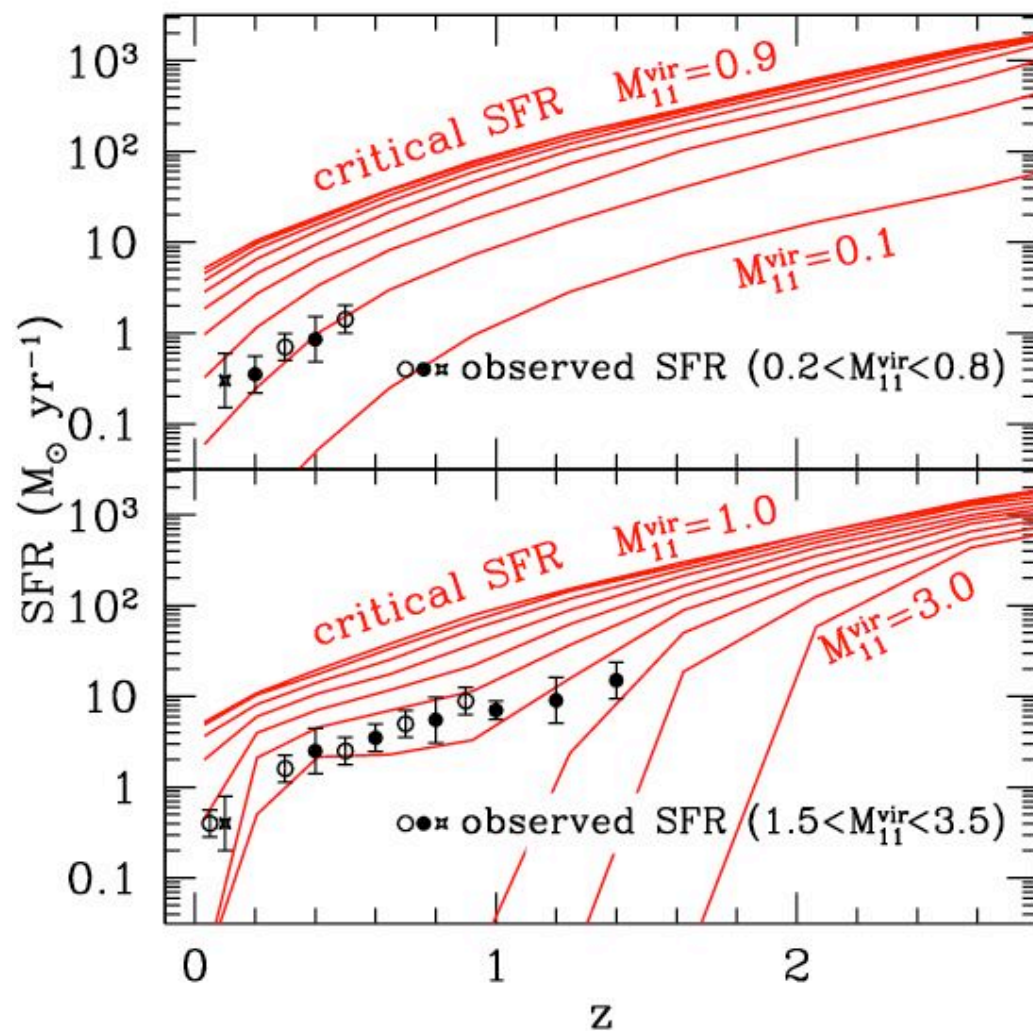
SC 2010

Effect on the Cooling time: hot-mode/cold-mode transition

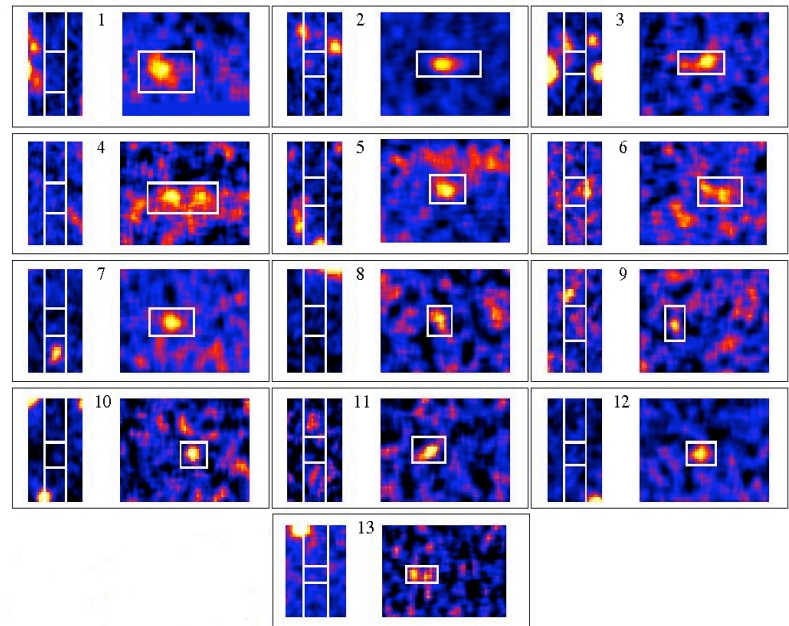
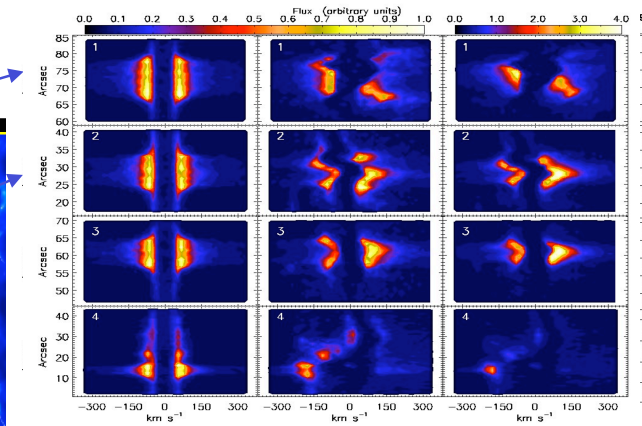
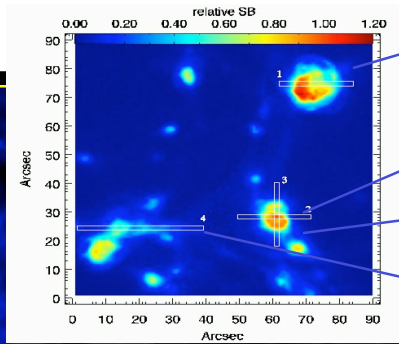


SC 2010

Implications on the evolution of the SFR



SC 2010



THE END

“always look at the bright side of the IGM!”

